DEVELOPMENT OF REDUCTIVE/OXIDATIVE TREATMENT STRATEGY FOR THE REMOVAL OF PER- AND POLYFLUOROALKYL SUBSTANCES (PFAS) IN WATER

by

AKSHAY CHANDRASHEKAR PARENKY

Presented to the Faculty of the Graduate School of

The University of Texas at Arlington in Partial Fulfillment

of the Requirements

for the Degree of

DOCTOR OF PHILOSOPHY

THE UNIVERSITY OF TEXAS AT ARLINGTON

August 2020

Acknowledgements

Firstly, I would like to thank my adviser Dr. Hyeok Choi for his continuous support and guidance through the journey of my Ph.D. His valuable insights and his organized approach to challenges have enabled me to tackle many problems in an efficient and timely manner.

I would also like to thank the members of my committee Dr. Melanie Sattler, Dr. Srinivas Prabakar, and Dr. Junha Jeon for their valuable questions and comments, as well as the staff and other faculty of the Civil Engineering Department at The University of Texas at Arlington (UTA). Their assistance and dedication to their duties has allowed me, and so many other students, to successfully earn our degrees.

I would also like to thank my colleagues Naomi Gevaerd de Souza, Wasiu Lawal and Nusrat Jahan Chaudhary for their friendship and enthusiasm during our time in the laboratory. My brother and my parents have been a source of inspiration,love, and support through this journey and I will always be grateful to them.

Finally, I would like to recognize the financial support received from Department of Defense through the Strategic Environmental Research and Development Program, Water Research Foundation through the Unsolicited Research Program, and UTA through the Interdisciplinary Research Program.

July 28, 2020

Abstract

DEVELOPMENT OF REDUCTIVE/OXIDATIVE TREATMENT STRATEGY FOR THE REMOVAL OF PER- AND POLYFLUOROALKYL SUBSTANCES (PFAS) IN WATER

Akshay Chandrashekar Parenky, PhD

The University of Texas at Arlington, 2020

Supervising Professor: Hyeok Choi

The detrimental health effects of halogenated compounds in humans has been well documented, and the frequent occurrence of per- and polyfluoroalkyl substances (PFAS) in the water environment is a recent global concern. Feasible and sensible treatment strategies are in dire need for environmental remediation and water treatment. Currently, efficient treatment is only obtained at a small scale and at a high energy cost.

This research is presented in three subsections, where decomposition of selected PFAS was evaluated under advanced oxidation techniques. The first study involved decomposition of a polyfluoroalkyl substance, 6:2 fluorotelomer sulfonate (6:2 FTS), in which 2 carbons of the alkyl chain are hydrogenated making the molecule more vulnerable to degradation. The 6:2 FTS was tested against some of the common oxidants such as persulfate (PS), peroxymonosulfate and hydrogen peroxide. Interestingly, 6:2 FTS was degraded by PS alone under ambient conditions. Several byproducts and fluoride release were observed and quantified. A decomposition pathway was proposed, and certain reaction intermediates were identified.

Upon achieving successful degradation of 6:2 FTS, a highly oxidized perfluorinated compound, perfluoroctanesulfonic acid (PFOS) was investigated. The absence of C-H bonds makes the molecule more resilient to conventional oxidation, hence a synergistic approach of using reduction combined with advanced oxidation was envisioned. This strategy involved the use of electrons generated by zero valent iron as the reductive source in combination with highly reactive radical species such as sulfate radical and hydroxyl radicals as the oxidizing species. This combination of oxidation and reduction was evaluated under several conditions by changing factors such as concentration, pH, and temperature. Significant removal of PFOS was observed in most cases but no transformation was observed. However, when this system was tested for perfluorooctanoic acid (PFOA), decomposition byproducts were observed consisting of short chain compounds demonstrating the potential for this treatment strategy.

Although decomposition of PFOA was achieved through the synergistic approach, the constraints of heat requirement reduce the practical applicability of the system. Since oxidants can be activated efficiently by transition metals, several different combinations of metal-oxidants were evaluated. Amongst these combinations, silver-PS was successful in decomposing a variety of carboxylic PFAS under ambient conditions without the use of any external energy source such as heat, ultra-violet or microwave. Significant byproduct and fluoride release were observed upon decomposition of selected PFAS. This system shows great potential for in situ application of PFAS remediation. The reaction mechanism for the system is complex and future studies should: i) investigate the role of silver and identify the reactive species responsible for the reaction, ii) identify an appropriate metal-oxidant pair capable of decomposing sulfonic PFAS, and iii) evaluate the efficacy of these systems for a wider range of PFAS.

Table of Contents

List of Figures

List of Tables

Chapter 1

Introduction

1.1 PFAS Properties and Occurrence

Per- and polyfluoroalkyl substances (PFAS) have been manufactured since the late 1950s.These compounds contain the second single strongest covalent bond of C-F (Smart, 1994). This fluorination process gives the molecule hydrophobic and oleophobic properties (Kissa, 1994). The structure of PFAS generally contain a hydrophobic C-F chain with a hydrophilic head as shown in the ubiquitous molecules perfluorooctanoic acid (PFOA) and perfluorooctanesulfonic acid (PFOS) in Fig 1-1.

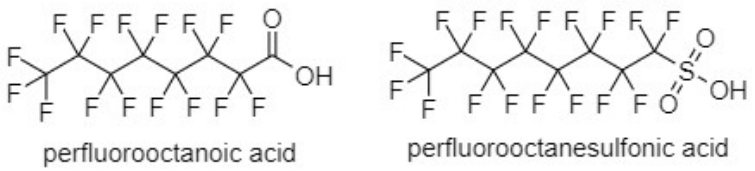

Figure 1-1: Chemical structure of PFOA, PFOS and with a perfluorinated, hydrophobic alkyl chain bonded to a hydrophilic functional group such as a carboxylic acid (PFOA) or a sulfonic acid (PFOS).

PFAS are a wide class of compounds which encapsulates nearly 6,000 compounds varying in different carbon chain lengths and functional groups; the properties of each compound are based on factors such as the carbon chain length, functional group and presence of hetero atoms (Buck et al., 2011). These compounds were both manufactured and imported from other countries into the United States for its application in a variety of products, with a total amount of PFAS imported between the years 1986 and

2005 ranging from 4.54 - 227 tons/year (Wang et al., 2014). Among these compounds PFOA and PFOS are the most prevalent and most studied of the PFAS (Wang et al., 2014). Their properties are listed in the Table 1-1 below, adapted from Kucharzyk et al. (2017).

Table 1-1: Physical and chemical properties of PFOA and PFOS (adapted from Kucharzyk et al., (2017)).

Property	**PFOS (potassium salt)**	**PFOA (free acid)**
Chemical Abstract Service (CAS) Number	2795-39-3	335-67-1
Physical description (at room temperature and pressure)	White powder	White powder
Molecular weight (g/mol)	538	414
Water solubility at 25 °C (mg/L)	550 to 570 (purified) 370 (fresh water) 25 (filtered sea water)	9.5×10^3 (purified)
Melting point (°C)	400	45 to 54
Boiling point (°C)	Not measurable	188 to 192
Vapour pressure at 20 °C (mm Hg)	2.48×10^{-6}	0.017
Octanol-water partition coefficient (log K_{ow})	Not measurable	Not measurable
Henry's constant (atm-m^3/mol)	3.05×10^{-9}	Not measurable
Half-life	Atmospheric: 114 days Water: > 41 years (at 25 °C)	Atmospheric: 90 days Water: > 92 years (at 25 °C)

Polyfluorinated alkyls are also highly used and prevalent in the environment, particularly fluorotelomer compounds such as 6:2 fluorotelomer sulfonate (6:2 FTS, shown in Fig. 1-2) that contain hetero atoms such as hydrogen on the carbon chain which makes it susceptible to microbial degradation (Hamid et al., 2020).

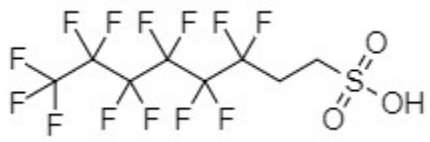

Figure 1-2: Chemical structure of 6:2 FTS.

Meanwhile, polyfluoroalkyl substances when subjected to degradation can form perfluorinated alkyls, e.g., treatments such as ozonation or treatment using sodium hypochlorite cause fluorotelomer to undergo transformation to form PFOA and PFOS (Xiao et al., 2018). As seen in Table 1-2 most of the carboxylic PFAS byproducts are formed as a product of degradation of commercially available hydrofluorocarbons (HFC) or hydrofluoroethers (HFE). When present in the environment in the oxidized form they are extremely hard to treat and rarely undergo any further transformation.

The use of PFAS is widespread including products such as non-stick cookware, food packaging, stain and water-resistant fabrics, and aqueous film forming foams (Kissa, 1994). At the end of these products life they are disposed of in landfills where through atmospheric changes, the PFAS in these compounds start leaching into the ground water and surrounding areas (Masoner *et al*., 2020). One of the most contaminated sites in the United States are military bases where regular fire-fighting sessions over several decades have contaminated the military bases with a plethora of PFAS, primary consisting of fluorotelomers (Milley *et al.,* 2018).

Table 1-2: Transformation of fluototelomers to terminal end products (adapted from Wang et al. (2014)).

Abbreviation (Commercial name)	CAS No.	Structure	Potential end-product (s)
HFC-247ccd	662-00-0	$CF_3(CF_2)_2CH_3$	PFBA
HFC 52-13p	335-37-3	$CF_3(CF_2)_4CHF_2$	C4-C6 PFCAs
N.A. (TH-8)	335-65-9	$CF_3(CF_2)_6CHF_2$	C4-C8 PFCAs
N.A. (TH-10)	375-97-3	$CF_3(CF_2)_8CHF_2$	C4-C10 PFCAs
HFC-76-13sf	80793-17-5	$CF_3(CF_2)_5CH_2CH_3$	C4-C7 PFCAs
THE-10	154478-87-2	$CF_3(CF_2)_9CH_2CH_3$	C4-C11 PFCAs

1.2 Exposure and Toxicity

The use of PFAS in the multitude of user end products, manufacturing sites, and fire-fighting foams leads to the exposure of these compounds through several different routes (Oliaei *et al.,* 2013). Exposure to these compounds can occur through direct contact such as using Teflon coated material or food packing materials. Whereas indirect exposure could be through leaching of PFAS from landfills into the ground water source (Roth *et al*., 2020; Lang *et al*., 2017) and uptake of PFAS from plants grown in waters contaminated with PFAS, it was also observed that sulfonic PFAS were adsorbed to a lesser extent than its carboxylic counterparts (Ghisi et al., 2019).

PFAS have also been detected in many sea creatures and land mammals across the world including some of the remotest regions of the artic (Ankley *et al.,* 2005; Giesy and Kannan 2001). Once ingested, PFAS do not undergo any metabolization which has led to significant increase in the levels of PFAS found in animals as well as in human blood

serum. The accumulation of PFAS was mainly observed in liver, kidney, and serum of rats (Chen and Guo 2009; Manzetti *et al*., 2014). In humans, PFAS are preferentially stored in the liver, and once entered, the half-life of PFOA and PFOS was determined to be respectively 3.8 and 5.4 years (ESFA, 2008). Moreover, in humans, it was noted that PFAS that settled over the proteins were transferred to the fetus through the maternal cord (Winkens *et al*., 2017).The toxicity of PFAS at different levels have been studied and PFOA is categorized as possible human carcinogen particularly for the kidney and testis, but other toxic effects also include thyroid disease and pregnancy related hypertension (IARC, 2016).

1.3 Treatment Strategies

The increasing prevalence of PFAS in surface waters, soil and living organisms calls for the development and implementation of efficient remediation strategies. The treatments currently available can be broadly classified into removal and decomposition technologies. Removal technologies include granular activated carbon (GAC), ion exchange and membrane filtration (Merino et al., 2016). The large surface area and pores present in the GAC make for excellent adsorbent materials has been demonstrated to remove a wide variety of PFAS from contaminated media and is currently being used to treat PFAS in drinking water treatment plants (Belkouteb et al., 2020). Ion exchange resins are another type of adsorbent material that can remove PFAS of various carbon chain lengths and have shown to be more effective than GAC for treating short chain PFAS (Maimaiti et al., 2018). Other novel adsorbents include alumina and amine-based absorbents such as cyclodextrin. The effectiveness of the these material highly rely on the matrix was the water to be treated, e.g., higher dissolved organic matter in water significantly hinders the adsorption process of the GAC and greater concentration of soluble ions impairs the

adsorption process of ion exchange resins (Ateia et al., 2019). While these technologies effectively remove PFAS from the contaminated media, the fate of the spent material is challenging to deal with due to the recalcitrant nature of the contaminants. The disposal of spent activated carbon and ion exchange resins has been a challenge in recent years since decomposition of PFAS has not been fully developed (Gagliano et al., 2020).

It has been observed that perfluoroalkyl compounds are not decomposed through biological means and the lack of advanced treatment systems in waste-water treatment plants generally lead to higher detection of short chain PFAS while long chain PFAS such as PFOS tend to accumulate in sludge post treatment process (Eriksson et al., 2017). Decomposition of PFAS is particularly difficult due to the multiple C-F bonds present in the molecule that make them extremely stable. A common disposal technique is using incineration wherein concentrated PFAS stream and some of the PFAS laden material is incinerated at temperatures above 1000 ˚C to undergo thermal oxidation (Kucharzyk et al., 2017). In order to optimize the decomposition technology through heat treatment, calcium hydroxide at various temperatures ranging from 300-600 °C was investigated, nearly 80% decomposition of PFOS was observed at temperatures about 400 °C with a reaction time of 20 min (Wang et al., 2015). A study done by Wu et al. (2019) tested several different amendments at 350 °C to identify which of the amendments would yield the highest decomposition, and according their study it was found that the addition of sodium hydroxide was capable of decomposing PFOS to a great extent. It suspected that the hydroxide ion is capable of reductively defluorinating PFOS.

1.3.1 Chemical reduction strategies

Reduction of pollutants has long been a strategy for the removal and decomposition of contaminants including halogenated compounds. Microbial reduction of chlorinated

solvents such as trichloroethlyene (TCE) and trichloroethane (TCA) has been successfully applied in the field (Walton and Anderson, 1990). While this method has advantages, a disadvantage is the need for electron donors and slower reaction kinetics. Chemical reduction by zero valent state metals has been successful in decomposing more recalcitrant halo-POCs such as PCB (Choi et al., 2008). Amongst many zero valent state metals, zero-valent iron (ZVI) is one of the most used remediation tools for the removal and decomposition of persistent organic pollutants (Zhang et al., 2003). The readily available electrons on the valence shell of ZVI make for an excellent electron donor and decompose the compounds in its vicinity as seen in Eqs.1 and 2.

$$Fe^0 \rightarrow Fe^{2+} + 2e^- \quad (1)$$

$$RCl + H^+ + 2e^- \rightarrow RH + Cl^- \quad (2)$$

Simultaneously ZVI can also react with the oxygen in aqueous solutions to produce hydrogen peroxide (HP) as seen in Eq. 3. The HP can then be activated by the ferrous ion (Fe^{2+}) to produce hydroxyl radicals as seen in Eq. 4.

$$Fe^0 + O_2 + 2H^+ \rightarrow Fe^{2+} + H_2O_2 \quad (3)$$

$$Fe^{2+} + H_2O_2 \rightarrow Fe^{3+} + OH^- + OH\bullet \quad (4)$$

While ZVI can produce both reducing and oxidizing species, the reactivity of ZVI is dependent on the size of the particles, (Fu et al., 2014)). The higher surface area promotes rapid oxidation of the ZVI surface to generate electron and radicals. Halo-POCs such as TCE and polychlorinated biphenyl (PCB) have been effectively degraded through dehalogenation process by ZVI and commonly used for in situ remediation (Choi et al.,

2009). Several modifications to ZVI such as coating it with magnesium aminoclay have evaluated for the removal and decomposition of contaminants including PFAS (Arvaniti et al., 2015).

1.3.2 Advanced oxidation techniques

The use of oxidants has been extensive for environmental remediation and some of the commonly used oxidants include hydrogen peroxide (HP), peroxymonosulfate (PMS) and persulfate (PS) (Wang and Wang 2018; Yang et al., 2020). Amongst these oxidants, PS has the highest redox potential of 2.01 V compared to HP and PMS. A common feature among these oxidants is the loosely bounded oxygen atoms in the molecule which upon cleavage can generate highly oxidizing radical species. Upon activation, these oxidants can produce highly oxidizing radical species such as hydroxyl radicals (•OH, HRs), sulfate radicals ($SO4^{\bullet-}$, SRs), and reducing radical species such as superoxide radical anions ($O2^{\bullet-}$, SRAs). The redox potential of SRs (E^0 = 2.6-3.1 V) are comparatively higher that HRs (E^0 = 1.9- 2.7 V) (Lee et al., 2020).

The amount and type of radical species generated are dependent on the activation method. For e.g., the number of SRs generated through UV are twice that generated though transition metals as seen in Eqs. 5 and 6 (Wang and Wang 2018).

$$S_2O_8^{2-} + h\gamma \rightarrow 2SO_4^{\bullet-} \quad (5)$$

$$S_2O_8^{2-} + Fe^{2+} \rightarrow SO_4^{\bullet-} + SO_4^{2-} + Fe^{3+} \quad (6)$$

Similarly, PMS can be activated using UV to generate both SRs and HRs as seen in Eq. 7.

$HSO_5^- + h\gamma \rightarrow SO_4^{\bullet -} + OH^{\bullet}$ (7)

Along with the activator, pH of the aqueous solution also plays a key role in the type of radical generated. Under alkaline conditions PS generates higher amounts of HRs than SRs. Similarly, HP generates SRAs under alkaline condition as shown in Eqs. 8-10 (da-Silva Rackov et al., 2016).

$H_2O_2 + Fe^{3+} \rightarrow HO_2^{\bullet} + Fe^{2+} + H^+$ (8)

$H_2O_2 + OH^{\bullet} \rightarrow HO_2 + H_2O$ (9)

$HO_2^{\bullet} \leftrightarrow O_2^{\bullet -} + H^+ \; pK_a = 4.8$ (10)

Each radical has a specific pathway of interaction leading to the decomposition of chemicals, e.g., SRs decompose chemicals through abstraction of an electron from the oxygen present in the carboxylic group, meanwhile HRs follow hydrogen abstraction to destabilize the molecule that eventually leads to its degradation (Lee et al., 2020). Although these methods can effectively activate the oxidants and degrade pollutants, the need for an external energy source greatly reduces in potential for in situ application. Hence, one of the most efficient ways of activating an oxidant is through the use of a transition metal. The classic Fenton reaction involves the generation of HRs by activating HP with dissolved Fe^{2+}. Modified Fenton reactions have evolved to use different activators with different oxidants. A study conducted by Anipsitakis and Dionysiu (2004) suggested that the best activator for PS was silver (I) whereas for PMS the best activator was cobalt (II).

1.4 Research Objectives

Objective 1: To evaluate the effect of hetero atoms in polyfluoroalkyl substances. The objective of this study was to investigate the transformation capability of polyfluoroalkyl substances containing C-H bonds. Conventional oxidation and advanced oxidation methods were implemented to evaluate the amount of transformation. To confirm this transformation, reaction byproducts had to be identified and fluoride release was to be observed. Moreover, a reaction pathway was to be proposed and reaction intermediates were to be identified.

Objective 2: To test the synergistic effect of ZVI and common oxidants for the removal and decomposition of PFOS. This study aims to evaluate the potential of PFAS treatment capability of the ZVI-based integrated system by checking if the system can synergistically remove and/or decompose PFOS in water. Batch experiments were conducted with ZVI and oxidants under various temperature, oxidant dose, and pH conditions, and results were discussed to propose possible mechanisms for the observed PFOS removal. PFOA was also briefly examined in comparison to PFOS

Objective 3: To identify the metal-oxidant pair capable of decomposing PFAS under ambient conditions. To achieve ambient condition degradation of PFAS, generation of highly reactive radical though modified Fenton reactions was investigated. Several transition metal-oxidant pairs were evaluated. Transition metals were used in their dissolved form to quickly activate the oxidants. Several parameters were modified to identify the appropriate metal-oxidant concentration. Once identified, PFAS containing different carbon chain lengths and functional groups were tested for its efficacy.

1.5 References

Anipsitakis, G. P., Dionysiou, D. D. (2004). Radical generation by the interaction of transition metals with common oxidants. Environ. Sci. Technol. 38 (13), 3705–3712.

Ankley, G.T., Kuehl, D.W., Kahl, M.D., Jensen, K.M., Linnum, A., Leino, R.L., Villeneuvet, D.A. (2005). Reproductive and Developmental Toxicity and Bioconcentration of Perfluorooctanesulfonate in a Partial Life-Cycle Test with the Fathead Minnow (Pimephales Promelas). Environ. Toxicol. Chem. 24(9), 2316-2324.

Arvaniti, O. S., Hwang, Y., Andersen, H. R., Stasinakis, A. S., Thomaidis, N. S., and Aloupi, M. (2015). Reductive degradation of perfluorinated compounds in water using Mg-aminoclay coated nanoscale zero valent iron. Chem. Eng. J. 262, 133-139.

Ateia, M., Arifuzzaman, Md, Pellizzeri, S., Attia M.F., Tharayli, N., Anker, J.N., Karanfil, T. (2019). Cationic polymer for selective removal of GenX and short-chain PFAS from surface waters and wastewaters at ng/L levels. Water Research. 163. 114874.

Belkouteb, N., Franke, V., McCleaf, P., Kohler, S., Ahrens, L. (2020). Removal of per- and polyfluoroalkyl substances (PFASs) in full-scale drinking water treatment plant: Long-term performance of granular activated carbon (GAC) and influence of flow-rate. Water Research. 182, 115913.

Buck, R.C., Franklin, J., Berger. U., Conder J.M., Cousins I.T., De Voogt, P., Jensen A.A., Kannan,K., Mabury, S.A., van Leeuwen, S.P.J. (2011). Perfluoroalkyl and Polyfluoroalkyl Substances in the Environment: Terminology, Classification, and Origins. Integr. Environ. Asses. 7 (4), 513–41.

Chen, Y.M., Guo, L.H. (2009). Fluorescence study on site-specific binding of perfluoroalkyl acids to human serum albumin. Arch. Toxicol. 83, 255–261.

Choi, H., Agarwal, S., Al-Abed, S. R. (2009) Adsorption and simultaneous dechlorination of PCBs by GAC impregnated with ZVI/Pd bimetallic particles: Mechanistic aspects and reactive capping barrier concept. Environ. Sci. Technol. 43, 488-493.

Choi, H., Al-Abed, S. R., Agarwal, S., Dionysiou, and Dionysios, D. (2008). Synthesis of Reactive Nano-Fe/Pd Bimetallic System-Impregnated Activated Carbon for the Simultaneous Adsorption and Dechlorination of PCBs. Chem. Mater. 20(11), 3649-3655.

Da Silva-Rackov, C. K. O., Lawal, W. A., Nfodzo, P. A., Vianna, M. M. G. R., do Nascimento, Claudio A. O., and Choi, H. (2016). Degradation of PFOA by hydrogen peroxide and persulfate activated by iron-modified diatomite. Appl. Catal. B_Environ. 192, 253-259.

Eriksson, U., Haglund, P., Karraman, A. (2017). Contribution of percursor compounds to the release of per- and polyfluoroalkyl substances (PFAS) from waste water treatment plants (WWTPs). J. Environ. Sci. 61, 80-90.

European Food Safety Authority, 2008. Opinion of the Scientific panel on contaminants in the food chain on perfluorooctane sulfonate (PFOS), perfluorooctanoic acid (PFOA) and their salts. EFSA J. 1–131.

Fu, F., Dionysiou, D.D., Liu, H.(2014). The use if zero-valent iron for groundwater remediation and wastewater treatment: A review. J. Haz. Mat. 267 (28). 194-205.

Gagliano, E., Sgroi, M., Falciglia, P.P., Vagliasindi, F.G.A., Roccaro, P. (2020). Removal of poly- and perfluoroalkyl substances (PFAS) from water by adsorption: Role of PFAS chain length, effect of organic matter and challenges in adsorbent regeneration. Water Research. 171, 115381

Ghisi, R., Vamerali, T., Manzetti, S. (2019). Accumulation of perfluorinated alkyl substances (PFAS) in agricultural plants: A review. Environ. Research. 169, 326-341.

Giesy, J.P., Mabury, S.A., Martin, J.W., Kannan, K., Jones, P.D., Newsted, J.L., Coady, K. (2006). Perfluorinated compounds in the Great Lakes. Environ. Chem. 5, 391-438.

Hamid, H., Li, L.Y., Grace, J.R. (2020). Aerobic Biotransformation of Fluorotelomer Compounds in Landfill Leachate-Sediment. Sci. Total Environ. 713, 136547.

IARC, (2017). MONOGRAPHS – 110. ⟨https://monographs.iarc.fr/list-of-classificationsvolumes/⟩.

Kissa, E. (1994). Fluorinated Surfactants. Dekker, NY: Marcel Dekker, Inc

Kucharzyk, K.H., Darlington, R., Benotti, M., Deeb, R., Hawley, E. (2017). Novel treatment technologies for PFAS compounds: A critical review. J. Environ. Manage. 204, 757-764.

Lang, J. R., Allred, B. M., Field, J.A., Levis, J.W., Barlaz, M.A. (2017). National Estimate of Per- and Polylfuoroalkyl (PFAS) Release to U.S. Municipal Landfill Leachate. Environ. Sci. Technol. 51, 2197-2205.

Lee, J., Von Gunten, U., Kim, J. (2020). Persulfate-Based Advanced Oxidation: Critical Assessment of Opportunities and Roadblocks. Environ. Sci. Technol.54,3064-3081. https://doi.org/10.1021/acs.est.9b07082.

Maimaiti, A., Deng, S., Pingping, M., Wang, W., Wang, B., Huang, J., Wang, Y., Yu, G. (2018). “Competitive adsorption of pefluoroalkyl substances on anion exchange resins in simluated AFFF-impacted groundwater”. J. Chem. Eng. 348, 494-502.

Manzetti, S., Roos van der Spoel, E., Van der Spoel, D. (2014). Chemical Properties, Environmental Fate, and Degradation of Seven Classes of Pollutants. Chem. Res. Toxicol. 27, 713-737.

Masoner, J.R., Kolpin, D.W., Cozzarelli, I.M., Smalling, K.L., Bolyard, S.C., Field, J.A., Furlong, E.T., Gray, J.L., Lozinski, D., Reinhart, D., Rodowa, A., Bradley, P.M. (2020). Landfill leachate contributes per-/polyfluoroalkyl substances (PFAS) and

pharmaceuticals to municipal wastewater. Environ. Sci. Water Res. Technol. 6, 1300.

Merino, N., Qu, Y., Deeb, R. A., Hawley, E. L., Hoffmann, M. R., and Mahendra, S. (2016). Degradation and removal methods for perfluoroalkyl and polyfluoroalkyl substances in water. Environ. Eng. Sci. 33(9), 615-649.

Milley, S. A., Koch, I., Fortin, P., Archer, J., Reynolds, D., Weber, K.P. (2018). Estimating the Number of Airports Potentially Contaminated with Perfluoroalkyl and Polyfluoroalkyl Substances from Aqueous Film Forming Foam: A Canadian Example. J. Environ. Manage. 222, 122–31.

Oliaei, F., Kriens, D., Weber, R., Watson, A. (2012). PFOS and PFC releases and associated pollution from a PFC production plant in Minnesota (USA). Environ. Sci. Pollut. Res. 20, 1977-1992.

Roth, J., Abusallout, I., Hill, T., Holton, C., Thapa, U., Haniga, D. (2020). Release of Volatile Per- and Polyfluoroalkyl Substances from Aqueous Film-Forming Foam. Environ. Sci. Technol. In press: https://dx.doi.org/10.1021/acs.estlett.0c00052.

Smart BE. Characteristics of C-F systems. In: Banks RE, Smart BE, Tatlow JC, editors. Organofluorine chemistry: Principles and commercial applications. New York (NY): Plenum; 1994. pp. 57–88.

Walton, B.T., Anderson T.A. (1990). Microbial Degradation of Trichloroethylene in the Rhizosphere: Potential Application to Biological Remediation of Waste Sites. App. Environ. Micro. 56 (4), 1012-1016.

Wang, Z., Cousins, I.T., Scheringer, M., Buck, R.C., Hungerbuhler, K. (2014). Global emission inventories for C4-C14 perfluoroalkyl carboxylic acid (PFCA) homologes from 1951to 2030, part II: The remaining pieces of the puzzle. Eviron. Intern. 69, 166-176

Wang, F., Lu, X., Li, X., Shih, K. (2015). Effectiveness and Mechanisms of Defluorination

of Perfluorinated Alkyl Substances by Calcium Compounds during Waste Thermal Treatment. Environ. Sci. Technol. , 5672-5680.

Wang, J., and Wang, S. (2018). Activation of persulfate (PS) and peroxymonosulfate (PMS) and application for the degradation of emerging contaminants. Chem. Eng. J. 334, 1502-1517.

Winkens, K., Vestergren, R., Berger, U., Cousins, I.T. (2017). Early life exposure to per- and polyfluoroalkyl substances (PFASs): a critical review. Emerg. Contam. 3, 55–68.

Wu, B., Hao, S., Choi, Y., Higgins, C.P., Deeb, R., Strathmann, T. (2019). Rapid Destruction and Defluorination of Perfluorooctanesulfonate by Alkaline Hydrothermal Reaction. Environ. Sci. Technol. Lett. 6, 630-636.

Xiao, F., Hanso, R.A., Golovko, S.A., Golovko, M.Y., Arnold, W.A. (2018). PFOA and PFOS are genertated from Zwitterionic and Cationic Precursor Compounds During Water Disinfection with Chlorine or Ozone. Environ. Sci. Let. 5, 382-388.

Yang, L., He, L., Xue, J., Ma, Y., Xie, Z., Wu, L., Huang, M., Zhang, Z. (2020). Persulfate-based decomposition of perfluorooctanoic acid (PFOA) and perfluorooctane sulfonate (PFOS) in aqueous solution: Review on influence, mechanism and prospective. J. Hazard. Mater. 393: 122405.

Zhang, W. (2003). Nanoscale iron particles for environmental remediation: An overview. J. Nano. Res. 5, 323-33.

Chapter 2

Room temperature oxidative transformation of 6:2 fluorotelomer by persulfate

2.1 Introduction

Per- and polyfluoroalkyl substances (PFAS) have been detected in water, soil, and air at alarming concentrations around the world (Mejia-Avendaño et al., 2020; Harrad et al., 2019; Milinovic et al., 2015). The hydrophobic and oleophobic properties of PFAS call for their numerous applications in water and oil repellents, non-stick cookware, food wrapping materials, and more importantly aqueous film forming foams (AFFFs) (Schaider et al., 2017; Herzke et al., 2012; Kissa, 1994). Due to their wide-spread presence and possible carcinogenicity, the United States Environmental Protection Agency (USEPA) has set an advisory limit for perfluorooctanoic acid (PFOA) and perfluoroctanesulfonic acid (PFOS) and designated them as national priorities (USEPA, 2018; USEPA, 2016), eventually forcing manufacturers to look for alternatives.

After the phase out of PFOS due to its notorious recalcitrance, a comparable PFAS containing 4 hetero atoms of hydrogen, known as 6:2 fluorotelomer sulfonate (6:2 FTS), has been widely used (Buck et al., 2011). Air force bases using AFFFs for fire-fighting drills have observed the highest level of PFAS in groundwater around them because 6:2 fluorotelomer sulfonamide alkylbetaine used as a major component of AFFFs degrades in the environment to various PFAS, particularly 6:2 FTS (Milley et al., 2018). Similarly, consumer products containing fluorotelomers end up in landfills where some of them are transformed, through microbial degradation, to perfluoroalkyl carboxylic acids (PFCA) and perfluoroalkyl sulfonic acids (PFSA) as terminal products (Hamid et al., 2020; Zhang et al., 2016). Consequently, various PFAS start leaching into nearby water resources and accumulating in plants and animals (Hoke et al., 2015).

There have been tremendous efforts to develop technologies for treatment of extraordinarily stable PFAS in the environment, particularly in water. As one of the most promising destructive methods, advanced oxidation technologies (AOTs) exploiting strong oxidizing radicals have been reported to decompose PFAS (Merino et al., 2016). Radicals, in particular sulfate radicals (SR; $SO_4^{\bullet-}$) and hydroxyl radicals (HR; $^{\bullet}OH$), can be practically generated from common chemical oxidants such as hydrogen peroxide (HP; H_2O_2), peroxymonosulfate (PMS; HSO_5^-), and persulfate (PS; $S_2O_8^{-2}$) when conjugated with transition metals so-called Fenton-like reaction (Anipsitakis and Dionysiou, 2004; Nfodzo and Choi, 2011a).

However, some PFAS, in particular PFAS in already highly oxidized forms such as PFOS and PFOA, strongly resist the radical attack under ambient conditions, (Parenky et al., 2020). In addition, decomposition of PFSA has been more challenging than that of PFCA because breaking C-S bond in PFSA needs a higher Gibbs free energy, thus requiring introduction of other supplementary energy sources such as ultraviolent (UV) radiation (Dos Passos Gomes et al., 2019). Similarly, most of PFAS are effectively decomposed upon modification of the Fenton-like reaction with non-radical mechanisms using photolysis, sonolysis, and thermolysis (Yang et al., 2020; Urtiaga et al., 2018; Vecitis et al., 2009). Heat-activated PS at high temperatures at around 60−90 °C was also reported to decompose exclusively PFCA such as PFOA but not PFSA such as PFOS (Yang et al., 2020; Bruton and Sedlak, 2018).

Consequently, decomposition of PFAS by the common oxidants alone under room temperature has been rarely reported. Herein, we report treatability of 6:2 FTS using the oxidants HP, PMS, and PS under ambient conditions, without introducing any other additional tools. Among many PFAS, 6:2 FTS was carefully selected considering the vulnerability of polyfluoroalkyl substances containing hetero atoms to radical attack

compared to perfluoroalkyl ones, along with its current widespread use and persistence. We hypothesize that the presence of C-H bonds in 6:2 FTS greatly increases the capability of oxidants to abstract those hydrogens, destabilizing 6:2 FTS and thus accelerating its further decomposition. This is the first demonstration of decomposition of 6:2 FTS at room temperature by common oxidants, leading to development of a more practical strategy to treat other PFAS similar to 6:2 FTS.

2.2 Materials and Methods

2.2.1 Chemicals and Materials

6:2 FTS (1H,1H,2H,2H fluorotelomer sulfonate, CAS 27619-97-2) was purchased from Synquest Labs (Alachua, FL). The isotopically marked internal standards for all parent and byproduct PFAS including PFOA, perfluoroheptanoic acid (PFHpA), perfluorohexanoic acid (PFHxA), perfluoroheptanoic acid (PFPeA), and perfluorobutanoic acid (PFBA) were purchased from Wellington Labs (Ontario, Canada). Sodium persulfate ($Na_2S_2O_8$), potassium peroxymonosulfate ($KHSO_5 \cdot ½KHSO_4 \cdot ½K_2SO_4$), ferrous sulfate heptahydrate ($FeSO_4 \cdot 7H_2O$), sodium hydroxide (NaOH), and sulfuric acid (H_2SO_4) were purchased from Sigma-Aldrich (St. Louis, MO). Acetonitrile (CAN; C_2H_3N), methanol (MeOH; CH_4O,), potassium iodide (KI), sodium bicarbonate ($NaHCO_3$), formic acid (CH_2O_2), tert-butyl alcohol (TBA), hydrogen peroxide (H_2O_2, 30% w/w), and fluoride ionic strength adjuster (ISA, Hach, Loveland, CO) were acquired from Thermo Fisher Scientific (Waltham, MA). Large molecule separation (LMS) cartridges were purchased from Agilent Technologies (Santa Clara, CA). All solutions and sample preparations were done in ultrapure water (18 MΩ·cm) produced by a Millipore Milli-Q filtration system (Billerica, Massachusetts).

2.2.2 Batch Experiment Setup

Batch experiments were conducted in propylene vials containing 10 mg/L of 6:2 FTS constituting a final volume of 20 mL. Standard concentration of oxidants was 0.3 M and ranged later at 0.3-0.03 M to examine the effect of PS dose. Solution pH started at around 6.5 after mixing all chemicals and was not controlled over reaction. To observe the effect of pH, solution pH was adjusted to 3.0 by adding 0.1 M of H_2SO_4 and 10.0 by adding 0.1 M of NaOH. The pH of the reaction did not change significantly over the course of the reaction in either acidic, neutral or basic conditions. For some selected experiments, Fe^{2+} as $FeSO_4$, targeting at 9 mM, was added to activate oxidants to accelerate the generation of radicals by the Fenton-like reaction. Scavenging experiments were also conducted by adding 0.3 mM of TBA or MeOH to quench the reactivity of produced radicals. All reactions were run for 8 h under ambient conditions (i.e., 20 °C and 1 atm).

2.2.3 Sample Treatment and Chemical Analysis

Sample collection, preparation and analysis was followed as described elsewhere (Parenky et al., 2020). In short, reaction samples of 0.2 mL drawn at predetermined time intervals were diluted in 1.8 mL of water, extracted with MeOH through pre-conditioned LMS cartridges in 1:1 ratio, and analyzed in a Shimadzu (Nakagyo-ku, Kyoto, Japan) Nexera liquid chromatograph (LC) mounted with an Agilent Zorbax Eclipse Plus C18 RRHD column (1.8 µm particle size) and coupled with a Shimadzu 8040 triple quadrupole mass spectrometer (MS). LC/MS analysis was conducted under gradient method using binary mobile phase of ACN and water injected with 0.1% CH_2O_2. For quantification of the target analyte 6:2 FTS and expected byproducts such as short-chain PFAS, multiple reaction monitoring scans were conducted in a negative electrospray ionization mode. Confirmation of expected reaction intermediates was undertaken using targeted analysis. Monitored ion

transitions for PFHpA, PFHxA, PFPeA, and PFBA were conducted as described by Bruton and Sedlak, (2018).

Aqueous fluoride ions (F^-) were measured by an Intellical ISE F121 electrode mounted to a Hach HQ 440D base (Loveland, CO) as shown in Fig. 2-1. Samples of 0.5 mL were diluted with 0.5 mL ISA stock solution (one pillow per 5 mL) prior to analysis.

Figure 2-1: Fluoride Intellical F121 electrode probe coupled to a Hach HQ 440D base.

Concentration of PS remaining in reaction solutions was traced using a spectrophotometric method as reported by Liang *et al.* (2008), where 0.5 mL sample was added to 4.5 mL of solution containing 100 g/L of KI and 5 g/L of $NaHCO_3$ and the resulting solution was read at 400 nm in a Shimadzu 2550 UV-visible spectrophotometer as seen in Fig 2-2.

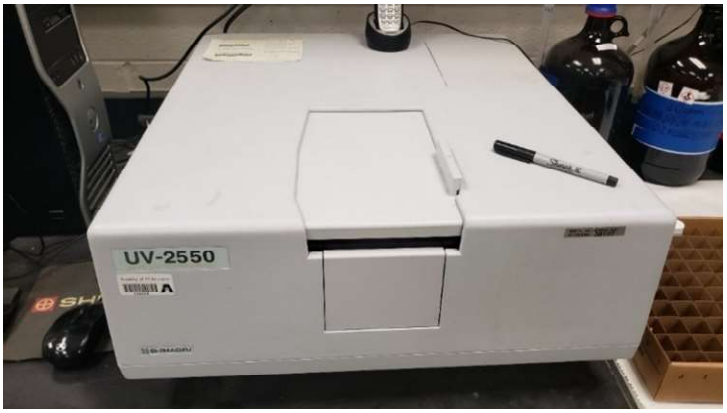

Figure 2-2: Shimadzu 2550 UV-visible spectrophotometer.

The total organic carbon was analyzed using a Shimadzu TOC-Vcsh shown in Fig. 2-3 in combination with a Shimadzu autosampler and nitrogen analyzer. Due to the high volume of samples required for the analysis, sacrificial batch reactors were kept for the various time intervals. Samples were placed in 20 mL autosampler vials and instrument was operated in the total carbon mode due to the absence of any inorganic carbon in the samples.

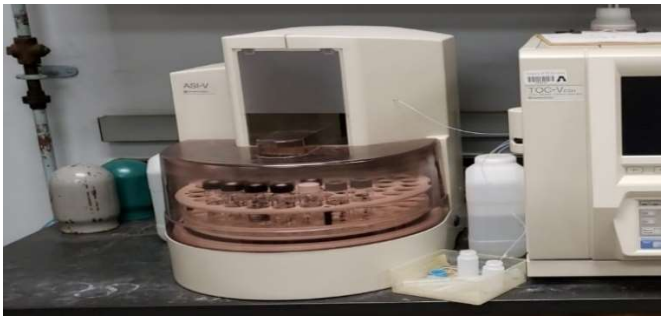

Figure 2-3: Shimadzu TOC-Vcsh analyzer.

2.3 Results and Discussion

2.3.1 Decomposition of 6:2 FTS by Oxidants

Three widely used oxidants were compared to decompose 6:2 FTS under ambient conditions, as shown in Fig. 1. As strong oxidants, they have high redox potentials (e.g., E^0 = 2.01 V for PS and E^0 =1.78 for HP) (Waclawek et al., 2017). Under specific conditions such as presence of electron donors, base-catalyzed reaction, and high temperatures, these oxidants are capable of generating SRs and HRs. Interestingly, HP was not able to decompose 6:2 FTS under the given conditions and thus negligible amounts of aqueous F- and reaction byproducts were detected. Meanwhile, the two sulfur-centered oxidants PS and PMS worked for decomposition of 6:2 FTS, producing significant amounts of F- and reaction byproducts (will be discussed later). Particularly PS showed much greater reactivity with 6:2 FTS, resulting in complete decomposition of 6:2 FTS in 6 h. PS is the strongest oxidizing agent in the peroxide family (i.e., redox potential E^0 = 2.01 V for PS, E^0 = 1.4 V for PMS, and E^0 = 1.70 V for HP) (Wacławek et al., 2017). Dependency of organic chemical decomposition on oxidant type has been also reported (Nfodzo and Choi, 2011a; Anipsitakis and Dionysiou, 2004).

In the previous study on PFOA and PFOS decomposition, the direct oxidation of the PFAS by oxidants alone has been reported to be ineffective, proposing needs of higher temperatures and/or transition metals (Parenky et al., 2020). PFOA and PFOS are perfluorinated alkyl substances with no C-H bonds while 6:2 FTS is a polyfluorinated alkyl with 4 C-H bonds. The observed decomposition of 6:2 FTS by PS and PMS alone, as shown in Fig. 2-4, suggests that the presence of hydrogen and thus C-H bonds along the alkyl chain makes 6:2 FTS more vulnerable to oxidative degradation.

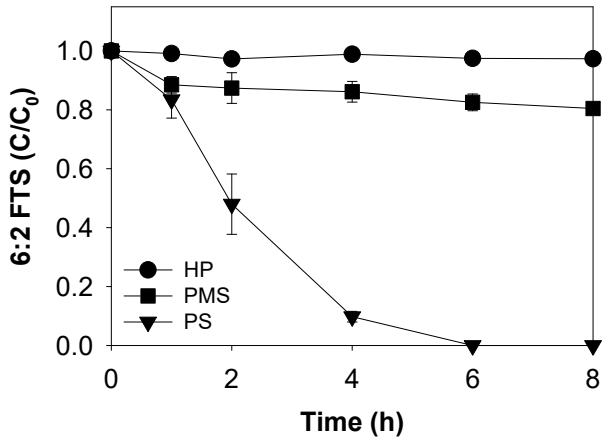

Figure 2-4: Decomposition of 6:2 FTS by various oxidants at room temperature (10 mg/L 6:2 FTS; 0.3 M oxidant; 20 °C; initial pH 6.5 to final pH around 5 (no pH control)). The error bars are the standard deviation of triplicated results.

2.3.3 Effects of PS Dose and Reaction pH

Since PS showed best reactivity with 6:2 FTS, the effect of PS dose on decomposition of 6:2 FTS was investigated in Fig. 2-5. The reaction kinetic was improved upon increase in PS dose from 0.03 to 0.30 M. In the previous experiments, pH was not controlled in order to observe the reactivity in the absence of any potential inhibition by buffer species. Initial pH at around 6.5 decreased to around 5 over 8 h. Then, in order to investigate the effect of reaction pH on decomposition of 6:2 FTS by PS, two more conditions were set up at pH 3.0 and 10.0 in either 0.1 M H_2SO_4 or 0.1 M NaOH buffer solution, as shown in Fig. 2-6. Neutral pH 6.5 showed 100% decomposition of 6:2 FTS while acidic pH 3 and basic pH 10 showed only at 19% and 53%, respectively.

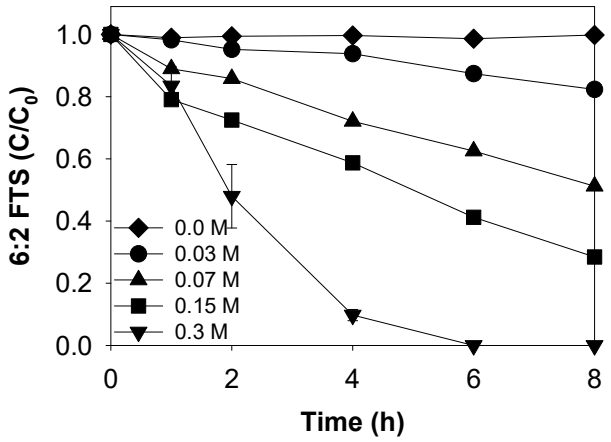

Figure 2-5:Decomposition of 6:2 FTS by PS at different concentrations (10 mg/L 6:2 FTS; 0.0-0.3 M PS; 20 °C; initial pH 6.5 to final pH around 5 (no pH control).

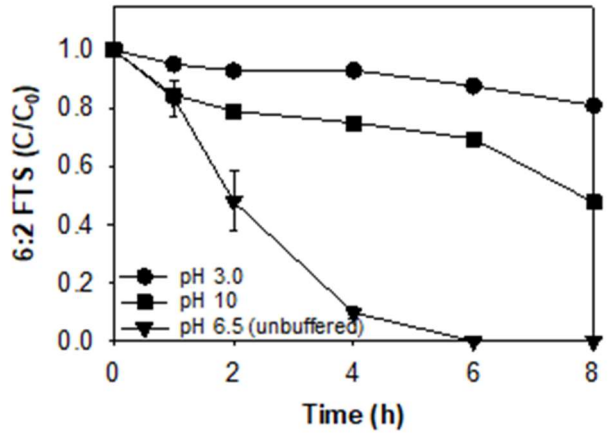

Figure 2-6: Decomposition of 6:2 FTS by PS under different pHs (10 mg/L 6:2 FTS; 0.3 M PS; 20 °C; initial pH at around 3.0, 6.5, and 10 to around 3.0, 5 and 9.7 respectively (buffer used only for pH 3.0 and 10)).

Along with actual pH impact, many other factors such as reaction of PS with buffering species used to control pH might have influenced the result. Possible reason for the low decomposition at pH 3 could be due to the formation of non-reactive H_2SO_5 and

less reactive HP than PS (note Fig. 2-4), as shown in Eq. 11 and 12 (Kolthoff and Miller, 1951). Higher decomposition of 6:2 FTS at pH 10 than pH 3.0 can be ascribed to alkaline activation of PS to produce SRs and HRs for decomposition of 6:2 FTS as shown in Eqs. 13-15 (Olha et al., 2010).

$$H_2S_2O_8 + H_2O \rightarrow H_2SO_5 + H_2SO_4 \quad (11)$$

$$H_2SO_5 + H_2O \rightarrow H_2O_2 + H_2SO_4 \quad (12)$$

$$S_2O_8^{2-} + 2H_2O \rightarrow HO_2^- + 2\ SO_4^{2-} + 3\ H^+ \quad (13)$$

$$HO_2^- + S_2O_8^{2-} \rightarrow SO_4^{\bullet-} + SO_4^{\ 2-} + H^+ + O_2^{\bullet-} \quad (14)$$

$$SO_4^{\bullet-} + OH^- \rightarrow SO_4^{\ 2-} + OH^{\bullet} \quad (15)$$

Nonetheless, the reaction condition of neutral pH at around 6.5 under no pH control and without any extra ionic species can be beneficial for practical applications later.

2.3.4 Impact of addition of Fe^{2+} to PS on 6:2 FTS decomposition

Previously PS and PMS alone showed significant decomposition of 6:2 FTS. Then, Fe^{2+} (abundant and non-toxic) was added to the system for generating SRs and HRs though the Fenton-like reaction and thus, if any, accelerating 6:2 FTS decomposition, as shown in Fig. 2-7. Considering the dependency of generation of major radical species on pH, it should be noted that pH dropped from 6.5 to around 1.5 in this case while pH of 6.5 dropped to 5 in the case of oxidants only in Fig. 2-4. Although it is hard to directly compare the effects of Fe addition on the reactivity of oxidants due to the different pH behaviors, addition of Fe to HP slightly helped decomposition of 6:2 FTS by generating radicals and/or making pH acidic but no significant changes were made for PS and PMS. Particularly, the reactivity of PS conjugated with Fe^{2+} at changing pH from 6.5 to 1.5 in Fig. 2-7 seemed to rather

have a higher decrease compared to that of PS alone at pH 6.5 in Fig. 2-4. However, it was comparable to that of PS alone at pH 3 in Fig. 2-6.

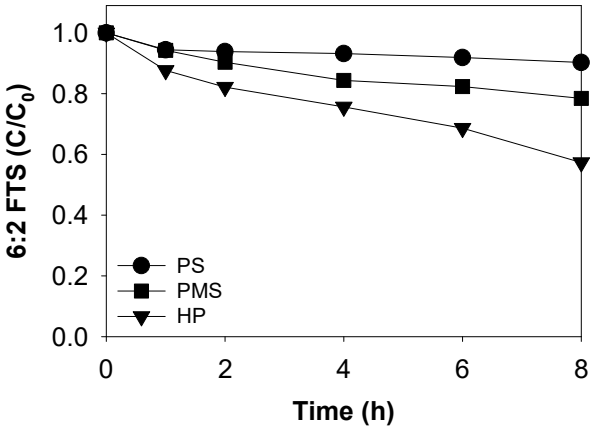

Figure 2-7: Decomposition of 6:2 FTS by various oxidants conjugated with Fe (10 mg/L 6:2 FTS; 0.3 M oxidant; 9 mM of Fe; 20 °C; initial pH 6.5 to final pH around 1.5 (no pH control)).

Activation of PS by Fe^{2+} yields radical species mostly such as SRs and HRs and similarly activation of HP by Fe^{2+} does HRs and superoxide radical anions (SRAs; O2•-) (Wang and Wang, 2020). Previously SRAs generated by HP activated by Fe-modified diatomite have demonstrated decomposition of PFOA (Da Silva-Rackov et al., 2016). The predominant radicals species generated are highly dependent on the reaction pH (Olha et al., 2010). Under the highly acidic condition tested in Fig. 2-7, the predominant species are speculated to be mostly SRs for PS/Fe^{2+}, SRs and HRs for PMS/Fe^{2+}, and HRs for HP/Fe^{2+} (Wang and Wang, 2020; Da Silva-Rackov et al., 2016; Olha et al., 2010). Based on the observed 6:2 FTS decomposition kinetics and the predominant species speculated, it is suggested that HRs work better than SRs for 6:2 FTS decomposition. Although the redox potential of HRs at E^0 = 2.7 V is slightly lower than SRs at E^0 = 2.8-3.0 V, they can easily

attack 6:2 FTS via hydrogen abstraction mechanism (Zhang et al., 2020). Methods of oxidation vary depending on the molecular structure of chemicals. For aliphatic chemicals like PFAS, HRs abstract mainly hydrogens in the chemicals while SRs abstract electrons from, e.g., oxygen in their functional group (Lee et al., 2020). Since the sulfur in 6:2 FTS is completely oxidized, it resists attack by SRs for electron abstraction. Meanwhile hydrogen in C-H bonds of 6:2 FTS is vulnerable to abstraction by HRs.

2.3.5 Evolution of F-, TOC, and Byproducts

Since significant decomposition of 6:2 FTS by PS alone at room temperature was observed in Fig. 2-4, we traced F- release, TOC reduction, and byproduct formation as direct evidence of its chemical defluorination, mineralization, and decomposition, as shown in Fig. 2-8. F- can be released by simple defluorination and/or complete mineralization. Interestingly, F- started being detected after at least 2 h, as shown in Fig. 2-8a. Since chemical defluorination, if any, typically occurs from the beginning of reaction while mineralization takes some time, the delayed release of F- implies that it is released by complete mineralization rather than chemical defluorination. In addition, no significant increase of F^- at 22% defluorination was observed after 6 h, suggesting possible exhaustion of PS at the time.

The change in total organic carbon (TOC) was monitored over the course of the reaction and shown in Fig. 2-8b. After 8 h, the total decrease in TOC was approximately 8% indicating the mineralization of 6:2 FTS. Formation of shorter chain PFAS as identifiable PFAS through the targeted LC-MS analysis was detected as shown in Fig. 2-8c. By PS at room temperature, 6:2 FTS was decomposed to PFHpA (C7), PFHxA (C6), PFPeA (C5), and PFBA (C4).

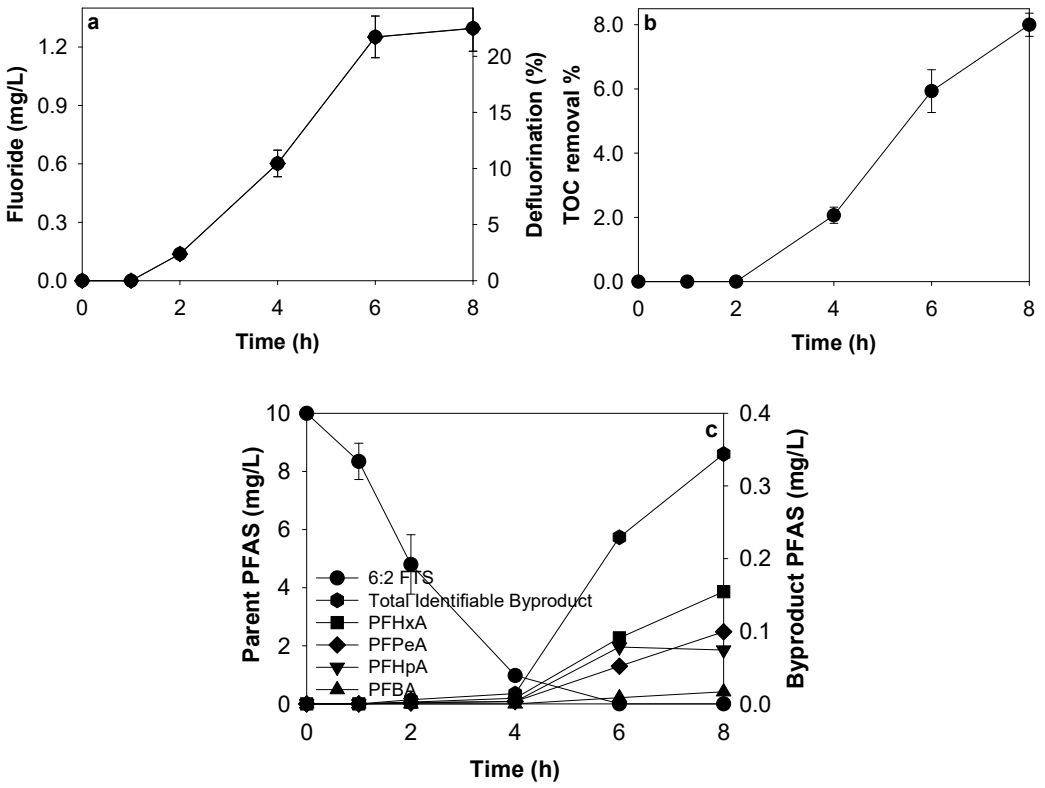

Figure 2-8: Evolution of (a) fluoride ion release, (b) TOC reduction, and (c) reaction byproduct formation during decomposition of 6:2 FTS by PS (10 mg/L 6:2 FTS; 0.3 M PS; 20 °C; constant pH at around 6.5 (no pH control)). Defluorination% is simply calculated based on observed F^- in water (note maximum F^- concentration, when all fluorines are detached, reaches 5.8 mg/L). F^- release is due to simple defluorination and complete mineralization of 6:2 FTS. Please note total identifiable byproducts count for only the limited number of short-chain PFAS byproducts (i.e., 4) among innumerable ill-defined byproducts.

Although significant decomposition of 6:2 FTS at 96% and its defluorination at 22% was observed for 8 h, total identifiable byproducts we targeted in the LC-MS analysis (i.e., sum of C4-C7) accounted for only 3.5%, implying formation of many other ill-defined

intermediates and byproducts as well as mineralization of 6:2 FTS as proven in Fig. 2-8b. Fortunately, formation of PFOS (C8) and PFOA (C8), which are more problematic due to their higher persistence, was not observed.

2.3.6 Possible Mechanisms and Pathways of 6:2 FTS Decomposition

Based on the experiments previously conducted, two possible reaction pathways were envisioned, 1 involving non-radical pathway while the other involving radical pathway. Experiments involving conventional and radical oxidation reactions yielded similar terminal byproducts. In order to find responsible reactive species among PS itself, HRs, and SRs, for the decomposition of 6:2 FTS, radical scavenger tests were carried out with TBA and MeOH to quench HRs and SRs, respectively, as seen in Fig. 2-9. At pH 6.5, no decomposition of 6:2 FTS was observed with MeOH while 6:2 FTS was significantly less decomposed only at 29% in the presence of TBA. The time required for the decomposition significantly increased (decomposition occurred after 24 hr, data not shown).

This suggested that the PS was interacting with the scavenger rather than 6:2 FTS itself. Based on these findings, the decomposition of 6:2 FTS was suspected to be through non-radical pathways. As seen in Fig. 2-10 the first step in the decomposition process is the cleavage of the C-S bond to simultaneous form 6:2 fluorotelomer alhdehyde (6:2FTAL) and 6:2 fluorotelomer alcohol. The 6:2 FTAL is later converted to 6:2 florotelomercarboxylic acid (6:2FTCA) which formed as major byproduct. Upon futher oxidation, the 6:2 FTCA is converted to PFHpA and 6:2 flurotelomer unsaturated acid though a loss of F-,which is then converted to 5:3 fluorotelomer carboxylic acid (5:3 FTCA) and 5:2 fluorotelomer ketone. The 5:3 FTCA is later converted to PFBA. Based on the quantification of byproducts a more favorable route is through transformation of 5:2 fluoroteolomer alcohol that is obtained from 5:2 fluorotelomer ketone to produce PFHxA and PFPeA. The highest

byproduct formation was observed for PFHxA followed by PFPeA. Similarly, these transformations could lead to mineralization It is important to note that the formation of the byproducts plateaued after 8 h suggesting that the byproducts were indeed terminal meaning that these byproducts were not further subjected to decomposition.

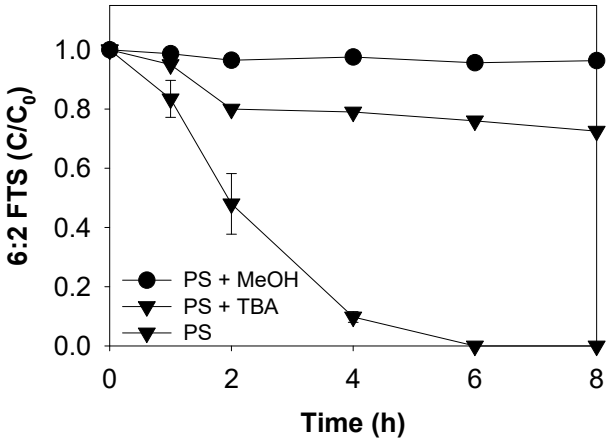

Figure 2-9: Decomposition of 6:2 FTS by PS in the presence of radical scavengers (MeOH and TBA) (10 mg/L 6:2 FTS; 0.3 M PS; 0.3 M scavenger; 20 °C; initial pH around 6.5 to final pH around 5 (no pH control)).

Although decomposition of 6:2 FTS was observed in Fe-oxidant system the transformation pathway is much harder to predict in the case of radical based degradation. Particularly, SRs played an important role in decomposing 6:2 FTS, but HRs also seemed to contribute to the decomposition in some extent. In fact, Nfodzo and Choi (2011b) proposed that SRs as an alternative to well-established HRs are very effective to decompose various persistent organic chemicals such pharmaceuticals.

SRs more selectively involve electron transfer in oxidation events because SRs have a higher oxidation potential at 2.3 V than HRs at 2.1 V (depending on pH), making

them a slightly better species for the direct electron transfer for PFAS decomposition than HRs (Buxton et al. 1988; Neta et al. 1988; Neta et al. 1977). SRs have previously been studied for the decomposition of PFOA (Da Silva-Rackov et al., 2016). The fact that PS and PMS as sulfur-centered oxidants are known to mostly generate SRs while HP generate HRs supports the observed result in Fig. 2-4. However, the reactivity of PS also greatly depends on reaction pH, generating different reactive radical species (Nfodzo et al., 2012).

It should also be noted that the reactivity of SRs and HRs varies upon the molecular structure of organic chemicals (Lee et al., 2020). PS has been proven to be effective for decomposition of polyaromatic hydrocarbon such as anthracene through generation of HRs under neutral to basic pHs and/or SRs under acidic pHs (Peluffo et al. 2016). Very similar result was reported by Bruton and Sedlak (2018), suggesting a systematic step-by-step removal of CF_2 moieties. When compared to CF_2 moieties removal as seen in PFOA degradation by SRs, it is speculated that the degradation of 6:2 FTS follows a different path where in reaction intermediates such as 6:2 fluorotelomer carboxylic acid, 5:2 fluortelomer ketone an 5:2 fluorotelomer alcohol is formed before transforming into PFHxA, PFPeA and PFBA. 5:2 fluorotelomer alcohol is formed before transforming into PFHxA, PFPeA and PFBA as reported by Shaw et al. (2019). Since the life of these intermediates is short, is was difficult to confirm the presence of these compounds and in turn confirm the reaction pathway but the proposed pathway could be a reasonable assumption since as seen through the reaction kinetics, even though 50% of the 6:2 FTS had disappeared no byproducts were observed until 4 hours suggesting the formation of many reaction intermediates such as the ones shown in Fig. 2-11.

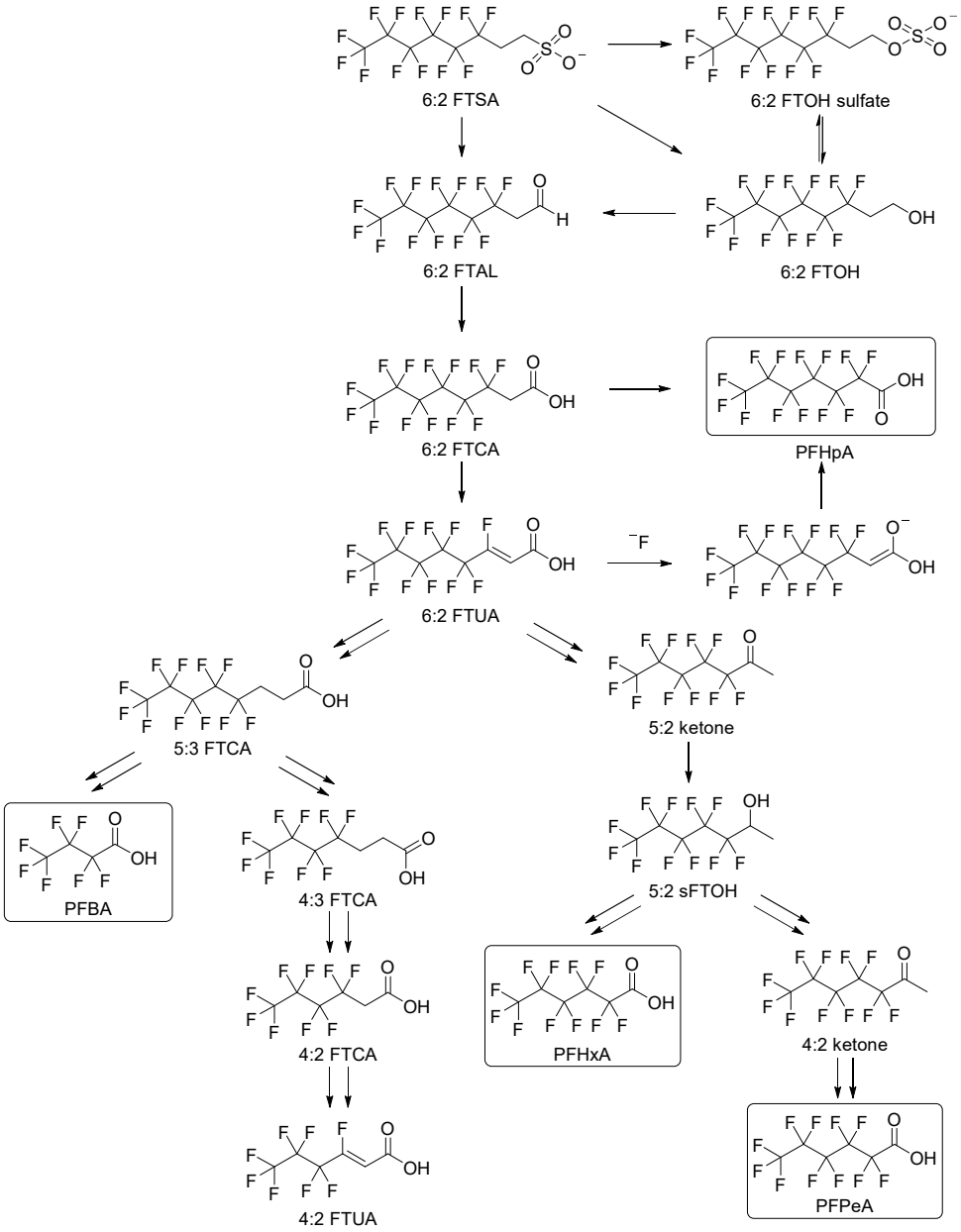

Figure 2-10: Proposed decomposition pathway of 6:2 FTS by PS alone under ambient conditions (10 mg/L 6:2 FTS; 0.3 M PS; 20 °C; initial pH 6.5 to final pH around 5 (no pH control).

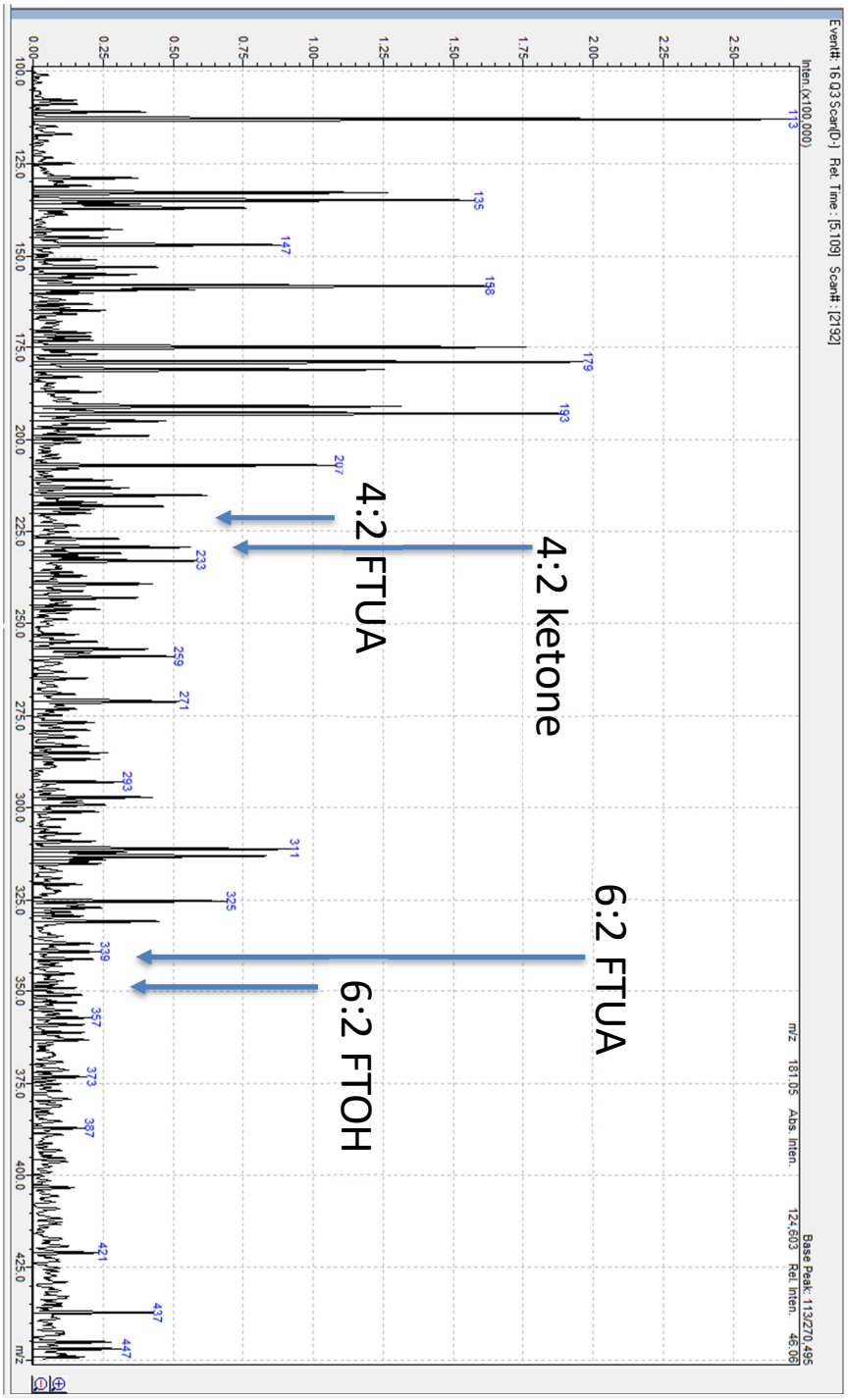

Figure 2-11: Reaction intermediates identified for the proposed decomposition pathway of 6:2 FTS by persulfate alone.

2.4 Conclusions

The potential of common oxidants (HP, PMS, and PS) to decompose 6:2 FTS containing 4 hetero hydrogen atoms was successfully demonstrated under ambient conditions. Sulfur-centered oxidants, in particular PS, were effective to decompose 6:2 FTS at pH around 6.5 under room temperature. In comparison to advanced oxidation, conventional oxidation exhibited higher and faster removal rates. Evolution of fluoride ion release and reaction byproduct formation such as short chain PFAS including PFBA (C4), PFPeA (C5), PFHxA (C6), and even PFHpA (C7) was confirmed. Decomposition of FTS was suspected to occur through non-radical based pathways. Some of the reaction intermediates were identified to confirm the proposed decomposition pathway.

2.5 References

Anipsitakis, G. P., Dionysiou, D. D. (2004). Radical generation by the interaction of transition metals with common oxidants. Environ. Sci. Technol. 38 (13): 3705–3712.

Bruton, T. A., Sedlak, D.L. (2018). Treatment of Perfluoroalkyl Acids by Heat-Activated Persulfate under Conditions Representative of in Situ Chemical Oxidation. Chemosphere 206, 457–64.

Buck, R.C., Franklin, J., Berger. U., Conder J.M., Cousins I.T., De Voogt, P., Jensen A.A., Kannan,K., Mabury, S.A., van Leeuwen, S.P.J. (2011). Perfluoroalkyl and Polyfluoroalkyl Substances in the Environment: Terminology, Classification, and Origins. Integr. Environ. Asses. 7 (4), 513–41.

Da Silva, C. K. O., Lawal, W. A., Nfodzo, P. A., Vianna, M., Do Nascimento, A., Choi, H. 2016. “Decomposition of PFOA by hydrogen peroxide and persulfate activated by iron-modified diatomite.” Appl. Catal. B: Environ. 192, 253-259.

Dos Passos Gomes, G., Wimmer, A., Smith, J.M., König, B., Alabugin, I.V. (2019). “CO2 or SO2: Should It Stay, or Should It Go?” J. Org. Chem. 84 (10), 6232–43.

Hamid, H., Li, L.Y., Grace, J.R. (2020). Aerobic Biotransformation of Fluorotelomer Compounds in Landfill Leachate-Sediment. Sci. Total Environ. 713, 136547.

Harrad, S., Wemken, N., Drage, D.S., Abou Elwafa Abdallah, M., Coggins, A.M. (2019). Perfluoroalkyl Substances in Drinking Water, Indoor Air and Dust from Ireland: Implications for Human Exposure. Environ. Sci. Technol. 53, 13449-13457. https://doi.org/10.1021/acs.est.9b04604.

Herzke, D., Olsson, E., Posner, S. (2012). Perfluoroalkyl and Polyfluoroalkyl Substances (PFASs) in Consumer Products in Norway - A Pilot Study. Chemosphere. 88 (8), 980–987. https://doi.org/10.1016/j.chemosphere.2012.03.035.

Hoke, R.A., Ferrell, B.D., Ryan, T., Sloman T.L., Green, J.W., Nabb, D.L., Mingoia, R.,

Buck, R.C., Korzeniowski, S.H. (2015). Aquatic Hazard, Bioaccumulation and Screening Risk Assessment for 6:2 Fluorotelomer Sulfonate. Chemosphere 128, 258–265.

Kissa, E. (1994). *Fluorinated Surfactants*. Dekker, NY: Marcel Dekker, Inc.

Kolthoff, I. M., Miller, I. K. (1951). The Chemistry of Persulfate. I. The Kinetics and Mechanism of the Decomposition of the Persulfate Ion in Aqueous Medium. J. Am. Chem. Soc. 73 (7), 3055–3059. https://doi.org/10.1021/ja01151a024.

Lee, J., Von Gunten, U., Kim, J. (2020). Persulfate-Based Advanced Oxidation: Critical Assessment of Opportunities and Roadblocks. Environ. Sci. Technol.54,3064-3081. https://doi.org/10.1021/acs.est.9b07082.

Liang, C., Huang C.F., Mohanty, N., Kurakalva, R.M. (2008). A Rapid Spectrophotometric Determination of Persulfate Anion in ISCO. Chemosphere 73 (9), 1540–1543.

Mejia-Avendaño, S., Zhi, Y., Yan, B., Liu, J. (2020). Sorption of Polyfluoroalkyl Surfactants on Surface Soils: Effect of Molecular Structures, Soil Properties, and Solution Chemistry. Environ. Sci.Technol. 54 (3), 1513–1521. https://doi.org/10.1021/acs.est.9b04989.

Merino, N., Qu, Y., Deeb, R.A., Hawley, E.L., Hoffmann, M.R., Mahendra, S. (2016). Degradation and Removal Methods for Perfluoroalkyl and Polyfluoroalkyl Substances in Water. Environ. Eng. Sci. 33 (9), 615–649. https://doi.org/10.1089/ees.2016.0233.

Milinovic, J., Lacorte, S., Vidal, M., Rigol. A. (2015). Sorption Behaviour of Perfluoroalkyl Substances in Soils. Sci. Total. Environ. 511, 63–71. https://doi.org/10.1016/j.scitotenv.2014.12.017.

Milley, S. A., Koch, I., Fortin, P., Archer, J., Reynolds, D., Weber, K.P. (2018). Estimating the Number of Airports Potentially Contaminated with Perfluoroalkyl and Polyfluoroalkyl Substances from Aqueous Film Forming Foam: A Canadian Example.

J. Environ. Manage. 222, 122–31.

Nfodzo, P., Choi, H. (2011a). Triclosan Decomposition by Sulfate Radicals: Effects of Oxidant and Metal Doses. Chem. Eng. J. 174, 629-634.

Nfodzo, P., Choi., H. (2011b). Sulfate Radicals Destroy Pharmaceuticals and Personal Care Products. Environ. Eng. Sci. 28 (8), 605–609.

Nfodzo, P., Hu, Q., Choi, H. (2012). Impacts of pH-Dependent Metal Speciation on the Decomposition of Triclosan by Sulfate Radicals. Water Sci. Technol. 12, 837-843.

Olha, F.S., Teel, A.L., Watts, R.J. (2010). Mechanism of Base Activation of Persulfate. Environ. Sci. Technol. 44 (16), 6423–28. https://doi.org/10.1021/es1013714.

Parenky, A.C., Gevaerd de Souza, N., Asgari, P., Jeon, J., Nadagouda, M. N., Choi, H. (2020). Removal of Perfluorooctanoic Acid in Water by Zero Valent Iron Particles Combined with Common Oxidants. Environ. Eng. Sci. (In Press, DOI: 10.1089/ees.2019.0406.

Schaider, L. A., Balan, S. A., Blum, A., Andrews, D. Q., Strynar, M. J., Dickinson, M.E., Lunderberg, D.E., Lang, J.R., Peaslee, G.F. (2017). Fluorinated Compounds in U.S. Fast Food Packaging. Environ. Sci. Technol. Lett. 4 (3), 105–111. https://doi.org/10.1021/acs.estlett.6b00435.

Shaw, D.M.J., Munoz, G., Bottos, E.M., Duy, S.V, Sauvé,S., Liu, J., Van Hamme, J.D. 2019. “Degradation and Defluorination of 6:2 Fluorotelomer Sulfonamidoalkyl Betaine and 6:2 Fluorotelomer Sulfonate by Gordonia Sp. Strain NB4-1Y under Sulfur-Limiting Conditions.” Sci. Total Environ. 647, 690–98.

Urtiaga, A., Soriano, A., Carrillo-Abad, J. (2018). BDD Anodic Treatment of 6:2 Fluorotelomer Sulfonate (6:2 FTSA). Evaluation of Operating Variables and by-Product Formation. *Chemosphere* 201, 571–77.

United States Environmental Protection Agency (USEPA). (2018). US Environmental Protection Agency, National Priorities: PER-AND POLYFLUOROALKYL SUBSTANCES (EPA-G2018-ORD-A1). Washington, DC: USEPA. Available at https://www.epa.gov/research-grants/national-priorities-and-polyfluoroalkyl-substances

United States Environmental Protection Agency (USEPA). (2016). *US* Environmental Protection Agency, Drinking Water Health Advisories for PFOA and PFOS (EPA-HQ-OW-2014-0138; FRL-9946-91-OW). Washington, DC: Office of the Federal Register, National Archives and Records Administration (NARA). Available at https://www.epa.gov/sites/production/files/2016-05/documents/2016-12361.pdf

Vecitis, C., Park, H., Cheng, J., Mader, B., Hoffman, M. (2009). Treatment technologies for aqueous perfluorooctanesulfonate (PFOS) and perfluorooctanoate (PFOA). Front. Environ. Sci. Eng. 3, 129-151.

Wacławek, S., Lutze, H. V., Grübel, K., Padil, V.V.T., Černík, M., Dionysiou. D.D. (2017). Chemistry of Persulfates in Water and Wastewater Treatment: A Review. Chem. Eng. J. 330, 44–62. https://doi.org/10.1016/j.cej.2017.07.132.

Wang, S., Wang, J. (2020). A Novel Strategy of Successive Non-Radical and Radical Process for Enhancing the Utilization Efficiency of Persulfate. Chemosphere. 245, 125555. https://doi.org/10.1016/j.chemosphere.2019.125555.

Yang, L., He, L., Xue, J., Ma, Y., Xie, Z., Wu, L., Huang, M., Zhang, Z. (2020). Persulfate-based decomposition of perfluorooctanoic acid (PFOA) and perfluorooctane sulfonate (PFOS) in aqueous solution: Review on influence, mechanism and prospective. J. Hazard. Mater. 393, 122405.

Zhang, S., Lu, X., Ning Wang, and Robert C. Buck. 2016. “Biotransformation Potential of 6:2 Fluorotelomer Sulfonate (6:2 FTSA) in Aerobic and Anaerobic Sediment.”

Chemosphere 154, 224–230.

Zhang, Y., Liu, J., Moores, A., Ghoshal, S. (2020). Transformation of 6:2 Fluorotelomer Sulfonate by Cobalt(II)-Activated Peroxymonosulfate. Environ. Sci Technol. 54 (7), 4631-4640. https://doi.org/10.1021/acs.est.9b07113.

Chapter 3

Zero valent iron conjugated with oxidants

3.1 Introduction

Per- and polyfluoroalkyl substances (PFAS) used in many industrial and military sectors and consumer products in our daily life, such as non-stick cookware, food packaging, stain and water-resistant fabrics, and aqueous film forming foams, have greatly contaminated the environment, particularly drinking water resources (Houtz et al., 2013; Kissa, 1994). Many of PFAS released into the environment undergo biological and environmental transformations eventually to the most oxidized state, i.e., perfluorooctanesulfonic acid (PFOS) and perfluorooctanoic acid (PFOA) (Eriksson et al., 2017; Dasu et al., 2013). Due to their widespread uses and bioaccumulative properties, PFOS and PFOA have been the most studied PFAS. The United States Environmental Protection Agency has set an advisory level in drinking water at 70 ng/L for them, and has designated PFAS as national priorities (USEPA, 2018; USEPA, 2016).

The carbon chain in PFOS and PFOA is surrounded by fluorine and attached with a functional group at the end, creating the hydrophobic and oleophobic property beneficial to many commercial products. The C−F bonds that PFAS contain (i.e., total of 17 in PFOS and 15 in PFOA) are known to be one of the strongest single covalent bonds in organic chemistry (note Fig. 8 later for the chemical structure of PFOS and PFOA). The C−F bonds are highly electronegative in nature, and cannot be oxidized easily (Merino et al., 2016; Vecitis et al., 2009). Most of PFAS are known not to be decomposed by conventional water treatment processes (Appleman et al., 2014). Advanced oxidation technologies (AOTs), which generate and exploit strong transient species such as hydroxyl radicals ($^{\bullet}OH$), sulfate radicals ($SO_4^{\bullet-}$), and superoxide radical anions ($O_2^{\bullet-}$) known to be highly effective for

decomposition of many persistent organic pollutants in water, might be useful in treating PFAS (da Silva-Rackov et al., 2016; Choi et al., 2010).

However, previous studies on AOTs showing successful decomposition of PFAS commonly employed an external energy source such as heat, ultraviolet, ultrasound, microwave, and electron beam to diminish the structural integrity of PFAS, rather than focusing solely on the generation of radical species for promoting chain reactions (Lyu et al., 2015; Park et al., 2011; Lee et al., 2010; Lee et al., 2009; Panchangam et al., 2009; Rayne and Forest, 2009; Dillert et al., 2007; Hori et al., 2007; Moriwaki et al.,2005; Hori et al.,2005; Hori et al., 2004). Among many AOTs, reactive species can be most practically generated through the Fenton (or Fenton-like) reactions, where transition metals such as iron (Fe) are used as a catalyst to activate oxidants including hydrogen peroxide (HP, H_2O_2), persulfate (PS, $S_2O_8^{2-}$), and peroxymonosulfate (PMS, HSO_5^-) for the generation of radicals such as $^{\bullet}OH$ and $SO_4^{\bullet-}$ (Bennedsen, 2014; Brillas et al., 1998; Ollis et al., 1991). The effectiveness of the Fenton reaction on decomposition of PFAS has been rarely reported probably because the C−F bonds in PFAS are relatively inert to the radicals.

Meanwhile, reduction of C−F bonds in PFAS might be thermodynamically possible. Previously, ZVI as a reducing agent has been popular to reductively decompose and thus dehalogenate many halogenated chemicals such as trichloroethylene and polychlorinated biphenyls (Zhang et al., 2017; Lefevre et al., 2016; Fu et al., 2014; Choi et al., 2008). However, no reports have shown successful defluorination of PFAS using ZVI alone under ambient conditions. Modification of ZVI or introduction of other similar mechanisms have been studied to improve the reaction kinetics (Lawal and Choi, 2019; Arvaniti et al., 2015). However, direct evidence for defluorination were not reported. When PFOS was subjected to extreme conditions (e.g., subcritical water at 350 °C), maximum reduction of PFOS was observed in the presence of ZVI (Hori et al., 2006). In general, chemical reduction or

defluorination, even if occurring under extreme conditions, results in defluorinated chemicals as final products which are more vulnerable to further chemical reactions via oxidation mechanisms.

Consequently, there have been efforts to generate various oxidizing and reducing species in combination to accelerate the decomposition of PFAS (Trojanowicz et al., 2018). In our recent study, successful decomposition of PFOA was achieved by combining oxidants and Fe-modified diatomite, where various radicals such as $SO_4^{\bullet-}$ as an oxidizing species and $O_2^{\bullet-}$ as a reducing species were generated (da Silva-Rackov et al., 2016). Considering the advantages and limitations of the oxidation pathway and the reduction pathway, we envisioned that combining the two complementary pathways might decompose PFAS more effectively.

In this current study, we conjugated ZVI with common oxidants such as HP, PS and PMS. ZVI as a strong reducing component released Fe^{2+} ions which activated added oxidants, while generating various oxidizing and reducing reactive species including free electrons, di-hydrogens, $O_2^{\bullet-}$, $^{\bullet}OH$, and $SO_4^{\bullet-}$ separately or in combination. The objective of this study was to evaluate the potential of PFAS treatment capability of the ZVI-based integrated system by quickly checking if the system can synergistically remove and/or decompose PFOS in water. Batch experiments were conducted with ZVI and oxidants under various temperature, oxidant dose, and pH conditions, and results were discussed to propose possible mechanisms for the observed PFOS removal. PFOA was also briefly examined in comparison to PFOS.

3.2 Experimental

3.2.1 Chemicals and Reagents

PFOS (heptadecafluorooctanesulfonic acid potassium salt, $C_8F_{17}SO_3K$, CAS 2795-39-3), PFOA (pentadecafluorooctanoic acid, $C_8F_{15}O_2H$, CAS 335-67-1), ferrous sulfate heptahydrate ($FeSO_4{\cdot}7H_2O$), ferric sulfate pentahydrate ($Fe_2O_{12}S_3{\cdot}5H_2O$), ferrous oxide (FeO), ferric oxide (Fe_2O_3), sodium borohydride ($NaBH_4$), sodium persulfate ($Na_2S_2O_8$), potassium peroxymonosulfate ($KHSO_5{\cdot}½KHSO_4{\cdot}½K_2SO_4$), sodium hydroxide (NaOH), and hydrochloric acid (HCl) were purchased from Sigma-Aldrich (St. Louis, MO). Acetonitrile (ACN, C_2H_3N), ethanol (C_2H_6O), methanol (CH_4O), sodium carbonate (Na_2CO_3-), sodium bicarbonate ($NaHCO_3$), formic acid (CH_2O_2), acetic acid ($C_2H_4O_2$), and hydrogen peroxide (H_2O_2, 30% in weight) were acquired from Fisher Chemical (Fair Lawn, NJ). All solutions and sample preparations were done in ultrapure water (18 MΩ·cm) produced by a Millipore Milli-Q filtration system (Billerica, Massachusetts). Commercially available ZVI, named reactive nanoscale iron particle (RNIP), was purchased from Toda Kogyo (Yamaguchi, Japan). All chemicals were used as received. Large molecule separation (LMS, 200 mg, 3 mL) and strong cation exchange (SCX, 200 mg, 3 mL) cartridges for solid phase extraction (SPE) were purchased from Agilent Technologies (Santa Clara, CA).

3.2.2 Synthesis and Characterization of ZVI

ZVI (boron-coated Fe) was synthesized through borohydride reduction of ferrous ions as described elsewhere (Liu et al., 2006). Briefly, 3 g of ferrous sulfate was dissolved in 4:1 (v/v) ethanol/water solution (90 mL) and mixed in a rotary shaker at 120 rpm to which 150 mL of 0.1 M sodium borohydride was added dropwise. ZVI was recovered by filtering the slurry with 0.45 μm glassfiber filter and washed with ethanol to remove any residual chemicals followed by methanol to prevent ZVI from oxidation. ZVI was submerged in

ethanol or methanol during its synthesis and stored in an air-tight vial, and thus oxidation of ZVI before its use was minimized. Then, ZVI was briefly characterized to confirm its properties. X-ray diffraction (XRD) using a Kristalloflex D500 diffractometer (Siemens, Munich, Germany) was used to investigate the crystallographic properties. The surface morphology was investigated using a Hitachi S-4800 II (Hitachi, Tokyo) scanning electron microscope (SEM) in combination with an energy dispersive X-ray spectroscopy (EDAX) while the overall morphology was observed using high resolution-transmission electron microscope (HR-TEM, JEOL JEM-2010F, Akishima, Tokyo). The size was determined using a SZ-100 particle size analyzer (Horiba Scientific, Irvine, CA). The surface area was determined using a Tristar 3000 (Micromeritics, Norcross, GA) porosimetry analyzer.

3.2.3 Batch Experiment

Reactions were carried in air-tight 20 mL polypropylene reaction vials containing a final volume of 20 mL with 10 mg/L PFOS (0.02 mM). Concentrations of oxidants were 0.3 M for PS and PMS, and 1.5 M for HP. Since salts such as PS and PMS greatly increase the ionic strength of the solution and pose analytical challenges for PFOS, PS and PMS were used in much lower concentrations than HP. These concentrations were also adopted from previous studies employing oxidants to decompose similar target compounds (Wang and Wang, 2018; da Silva-Rackov et al., 2016; Mitchell et al., 2014). ZVI concentration was 0.5 g/L.

Reaction temperature was fixed at 20 °C unless otherwise mentioned. Initial pH was controlled by using 2 M HCl or 2 M NaOH (in most of the tests, NaOH was needed to control pH because addition of the reactants decreased pH significantly). Buffer species were not used since they were expected to react with the radicals and to interfere with the analysis of PFOS. In order to investigate the effects of operational parameters, oxidant

doses were varied at 0.03 and 0.3 M for PS and PMS and 0.15 and 1.5 M for HP; temperature was controlled at 20, 40 and 60 °C; and initial pH was controlled at 3 (acidic), 7 (neutral), and 9 (basic). One experiment on a comparison basis to PFOS was conducted using PFOA under the same conditions. The reaction time for the batch setup was prolonged up to 48 h to observe possible reaction intermediates from the decomposition of PFOS and PFOA, if any.

PFOS removal potentially by adsorption to solid Fe_2O_3 and FeO particles under different initial pHs of 3, 7, and 9 was also attempted with 2 g/L Fe_2O_3 and 0.8 g/L FeO that resulted in 0.5 g/L as Fe. Instead of the Fe oxides, dissolved Fe^{3+} and Fe^{2+} ions were added to check for the possible complexation of PFOS with the Fe species. A proper amount of $FeSO_4 \cdot 7H_2O$ and $Fe_2O_{12}S_3 \cdot 5H_2O$ salt was added to achieve 0.25−2 g/L Fe^{3+} and Fe^{2+} under pH 3.

3.2.4 Sample Treatment and Chemical Analysis

Samples of 0.2 mL were diluted in 1.8 mL of ultra-pure water. LMS cartridges were preconditioned using 12 mL of methanol and washed with 12 mL of ultrapure water. Later, samples were extracted with methanol in a ratio of 1:1. The samples were analyzed in a Shimadzu (Nakagyo-ku, Kyoto, Japan) Nexera liquid chromatograph (LC) equipped with a Shimadzu 8040 triple quadrupole mass spectrometer (MS) as seen in Fig. 4-1. The flow rate was set at 0.8 mL/min with a binary gradient method. Mobile phase was 0.1% formic acid in water and in ACN. Separation was achieved by an Agilent Zorbax Eclipse Plus C18 column (1.8 µm particle size), and target analytes were eluted through a gradient method in which ACN was increased 5% to 100% over 6 min, kept at 100% for 3 min, and then brought down to 5% in 1 min. Column temperature was set at 40 °C, and sample injection was set at 10 µL.

Figure 3-1: Nexera LC equipped with a Shimadzu 8040 triple-quadrupole MS.

For quantification of the target analyte such as PFOS and PFOA and expected byproducts such as short-chain PFAS, multiple reaction monitoring (MRM) scans were conducted in a negative electrospray ionization mode. Confirmation of expected reaction intermediates was undertaken using targeted analysis. Monitored ion transitions of PFOS and other selected PFAS were conducted as shown in Table 4-1 adapted from Bruton and Sedlak (2017).

Table 3-1: Monitored transitions of selected PFAS in LC/MS equipment (adapted from Bruton and Sedlak (2017)).

Compound	Precursor Ion	Quantifier Product Ion	Qualifier Product Ion
PFOA	413	369	169
PFOS	499	80	99
PFHpA	363	319	169
PFNA	463	419	219
[$^{13}C_8$] PFOA	421	376	N/A
[$^{13}C_8$] PFOS	507	99	N/A
[$^{13}C_4$] PFHpA	367	322	N/A
[$^{13}C_9$] PFNA	472	427	N/A
[$^{13}C_4$] PFBA	217	172	N/A
[$^{13}C_5$] PFPeA	268	223	N/A
[$^{13}C_5$] PFHxA	318	273	N/A

To find any changes in the molecular structure of PFOS, particularly by defluorination, nuclear magnetic resonance spectrometry (NMR) analysis was carried out in a 300 Hz Oxford instrument (Abingdon, Oxfordshire, U.K). PFOS and intermediates were extracted using methanol in 1% acetic acid. Then, sample was evaporated using a rotovamp and later dissolved in 0.5 mL of deuterated methanol. For the identification of fluoride ions detached from PFOS, ion chromatography (IC) was employed using a Dionex (Thermofisher, Waltham, MA) DX–500 system shown in Fig.4-2 (theoretical concentration

of fluoride ions in water, when fully released, was 6.1 mg/L). SPE was conducted with SCX cartridges to extract fluoride ions. These cartridges were conditioned with 3mL methanol and equilibrated with 3 mL ultrapure water prior to loading 0.5 mL of the sample, which was then collected for analysis. The column used for the separation was a Dionex Ionpac AS-14A (4 mm × 250 mm) coupled with a Dionex Ionpac guard column AG-14A (4 mm × 50 mm). The eluent was 4.5 mM of sodium carbonate and 0.8 mM of sodium bicarbonate. An isocratic method with a flow rate of 1 mL/min was applied. A 4 mm Dionex AERS suppressor was employed to reduce background conductivity of the mobile phase.

Figure 3-2: Dionex DX-500 IC system.

3.3 Results and discussion

3.3.1 Characterization results

Characterization was done on freshly synthesized ZVI to confirm some of its properties. As seen in Fig. 3-3, the SEM image shows the morphology of the ZVI surface. Whereas in Fig.3-4 the EDAX report confirms the presence of iron with low oxide in the sample.

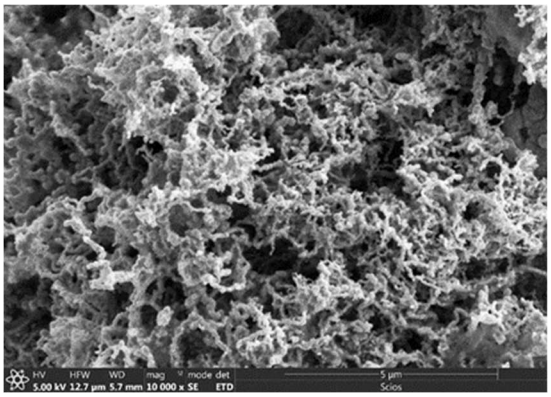

Figure 3-3: SEM image showing the surface morphology of freshly synthesized ZVI.

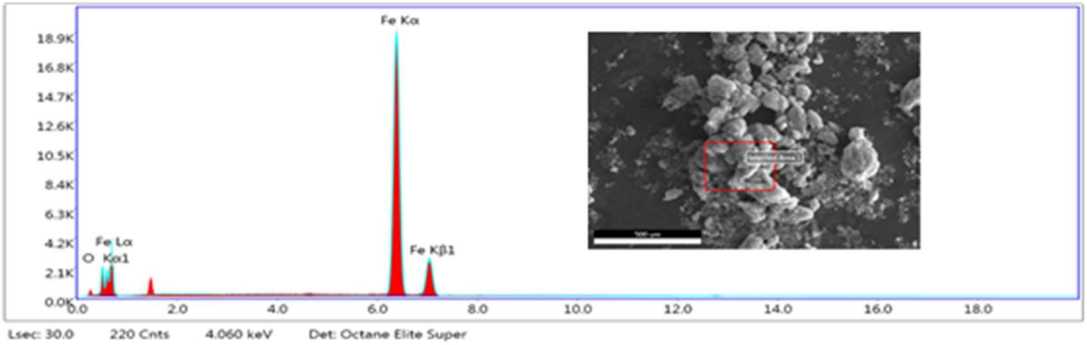

eZAF Smart Quant Results								
Element	Weight %	Atomic %	Net int.	Error %	K ratio	Z	A	F
O K	4.07	12.90	394.76	5.45	0.0273	1.0779	0.6223	1.0000
FeK	95.93	87.10	8986.30	1.07	0.8667	0.8944	1.0099	1.0003

Figure 3-4: SEM-EDX image of freshly synthesized ZVI indicating presence of elemental iron.

3.3.2 Reactivity of ZVI and RNIP

Prior to the batch experiment, we briefly characterized the home-made ZVI (herein, ZVI) synthesized via the well-established method to confirm that Fe particles in the samples are in zerovalent state and at nanoscale (trivial graphical data are not provided in this text). XRD results indicated the presence of ZVI at 2θ of 45°. HR-TEM showed ZVI nanoparticles in size of around 19 nm and RNIP in size of around 45 nm. Surface area of ZVI was 37.5 m^2/g while that of RNIP was 30 m^2/g. The properties were very close to those reported elsewhere (Choi et al., 2008; Liu et al., 2006).

Since hydrodehalogenation capability of ZVI has been well studied with persistent chemicals such as polychlorinated biphenyls (Choi et al., 2009a), the reactivity of both RNIP and ZVI was examined for defluorination of PFOS under standard conditions, as demonstrated in Fig. 3-5a showing aqueous concentration change of PFOS. RNIP was not able to significantly remove PFOS via reductive defluorination or even physical adsorption. Although the unique home-made ZVI, called boron-coated Fe, has been known to generate highly reactive di-hydrogen through reduction of water, which is involved in strong hydrodehalogenation reaction, no PFOS was removed. Accordingly, no fluoride ions were detected in the reaction samples, suggesting that ZVI alone lacks the capability to reductively defluorinate PFOS under the tested conditions. Although dehalogenation, particularly dechlorination by ZVI or many other zerovalent metals, has been thoroughly employed in environmental applications, defluorination of PFOS might be more challenging due to the absence of low-laying vacant d orbitals to accept an electron in PFOS. Recent studies also pointed out that defluorination of PFAS by ZVI-based materials is thermodynamically possible but kinetically negligible (Blotevogel et al., 2018; Park et al., 2018; Lawal and Choi, 2018).

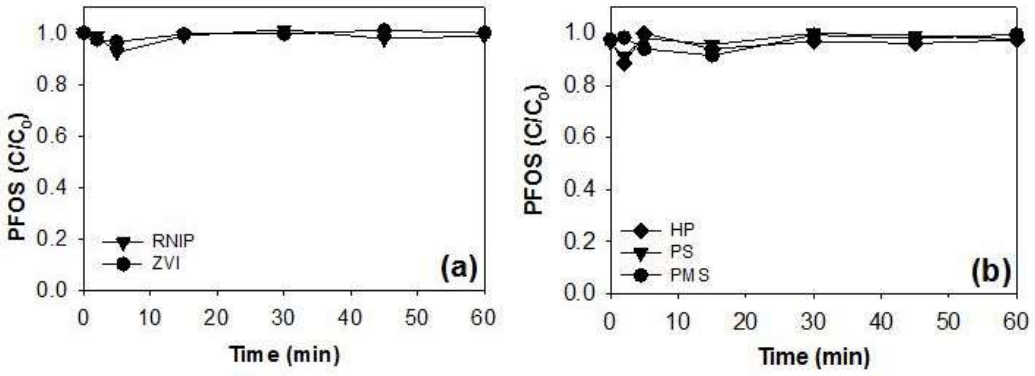

Figure 3-5: (a) PFOS removal by zerovalent iron (ZVI or RNIP) alone under standard conditions (10 mg/L PFOS; 0.5 g/L ZVI or RNIP; no oxidant; initial pH 7; 20 °C) and (b) PFOS removal by oxidant (HP, PS or PMS) alone under standard conditions (10 mg/L PFOS; no ZVI; 1.5 M HP, 0.3 M PS or 0.3 M PMS; initial pH 7; 20 °C). Note different concentrations for HP, PS, and PMS were used, as explained in the experimental section.

3.3.3 Reactivity of oxidants

To examine if oxidants alone can remove PFOS via the conventional oxidation pathway, the reactivity of each oxidant with PFOS was examined under standard conditions, as shown in Fig. 3-5b. Although HP, PS, and PMS have been widely used as strong oxidants to decompose a variety of chemicals (Bennedsen, 2014), none of them were able to decompose PFOS. The result was expected from the strength of the C−F bonds in PFOS and the absence of C−H bonds vulnerable to chemical reactions with the oxidants.

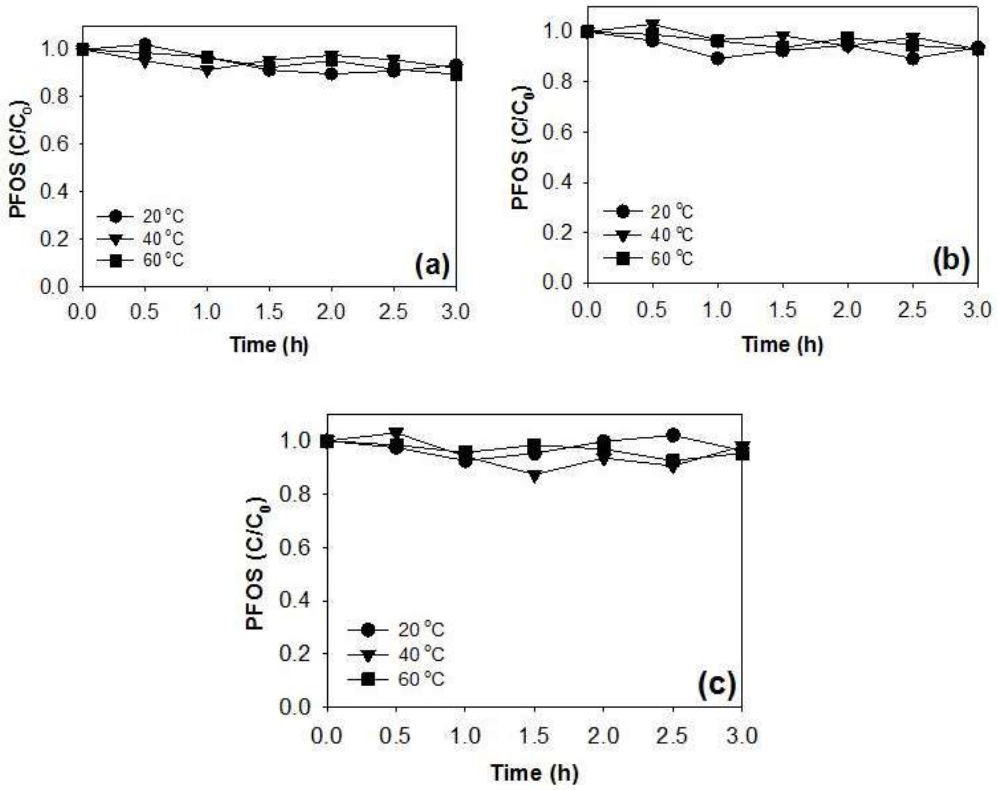

Figure 3-6: PFOS removal by oxidants alone (a) PS, (b) PMS, and (c) HP at different temperatures (10 mg/L PFOS; no ZVI; 0.3 M PS, 0.3 M PMS or 1.5 M HP; initial pH 3; 20, 40 or 60 °C).

It is known that oxidants can be activated more vigorously at high temperatures. Specifically, heat-activated PS has been successful in degrading many organic chemicals while other oxidants such as PMS and HP have been reported to be less or not affected by reaction temperature (Yang et al., 2010). The effect of temperature at up to 60 °C on the reactivity of oxidants with PFOS was tested, as shown in Fig. 3-6. Reaction time was expanded to 3 h and initial pH at 3.0 evolved to around 1.5 in the end. Interestingly, none of the conditions showed meaningful removal of PFOS. Decomposition by heat-activated PS (80 °C, pH < 3) has been reported exclusively for PFOA while decomposition of PFOS

has been reported at much lower or negligible rates (Bruton and Sedlak, 2018). Similarly, Park et al. (2016) also reported that PS alone under high temperatures oxidized PFOA but not PFOS. Oxidant activation temperature does not seem to impact on the decomposition of PFOS.

3.3.4 ZVI conjugated with oxidants

Since ZVI alone for defluorination or adsorption of PFOS and oxidants alone for oxidation of PFOS did not work, ZVI was conjugated with oxidants as shown in Figs. 3-7 to 3-9 to produce various oxidizing and reducing radicals including $^{\bullet}OH$, $SO_4^{\bullet-}$, and $O_2^{\bullet-}$. The home-made ZVI generally showing better performance than RNIP was used for all the following experiments. HP is known to generate mostly $^{\bullet}OH$ while PS and PMS generate mostly $SO_4^{\bullet-}$ (Oh et al., 2010; Anipsitakis and Dionysiou, 2004). Since PFOS does not contain C−H bonds, $^{\bullet}OH$ and $SO_4^{\bullet-}$ must work through electron transfer reaction rather than hydrogen abstraction reaction. Thus, $SO_4^{\bullet-}$ might be a better choice than $^{\bullet}OH$ for the decomposition of PFOS because $SO_4^{\bullet-}$ exhibit slightly higher redox potential than $^{\bullet}OH$ (depending on pH) for such electron transfer to PFOS (Wang and Wang, 2018; Anipsitakis and Dionysiou, 2004). Da Silva-Rackova et al., (2016) reported that $O_2^{\bullet-}$ as a strong reducing species generated from combination of oxidants and Fe ions were able to significantly remove PFOA. When ZVI is introduced, there is a slow release of electrons and Fe species as opposed to directly adding ferrous ions in the traditional Fenton reaction (Zhao et al., 2010). The slow release of Fe^{2+} and eventually Fe^{3+} ions might reduce scavenging of $SO_4^{\bullet-}$ and thus benefit degradation of organic chemicals (Watts et al., 2017; Rodriguez et al., 2014).

The ZVI-based integrated system was able to remove PFOS. As shown in Fig. 3-7 (please note the result only at 20 °C at this moment), PFOS removal was marginally

improved with the integrated systems when compared to oxidants or ZVI alone showing negligible removal of PFOS. The integrated systems of PS, PMS, and HP in the presence of ZVI presented 7%, 8%, and 12% PFOS removal, respectively.

3.2.5 Effects of Temperature, Oxidant Dose, and Reaction pH

Reaction conditions were adjusted to accelerate the PFOS removal kinetics and to elucidate the effects of operational parameters. Increased reaction kinetics was also believed to help to identify reaction intermediates and fluoride ions produced as a result of PFOS decomposition and thus to interpret any possible removal mechanisms. ZVI conjugated with PS was examined at different temperatures, as shown in Fig. 3-7a.

Interestingly, PFOS removal was much improved from 7% at 20 °C, 31% at 40 °C, to 54% at 60 °C, while there was no significant effect of temperature on the reactivity of PS alone shown in Fig. 2(a). It has been reported that higher temperatures increase the production of $SO_4^{\bullet-}$ in the Fenton reaction (Kim et al., 2018).

Figures 3-7b and 3-7c show ZVI conjugated with PMS and HP, respectively, demonstrating similar results to ZVI+PS. ZVI removed PFOS by 8% at 20 °C, 22% at 40 °C, and 53% at 60 °C with PMS and 12% at 20 °C, 59% at 40 °C, and 74% at 60 °C with HP.

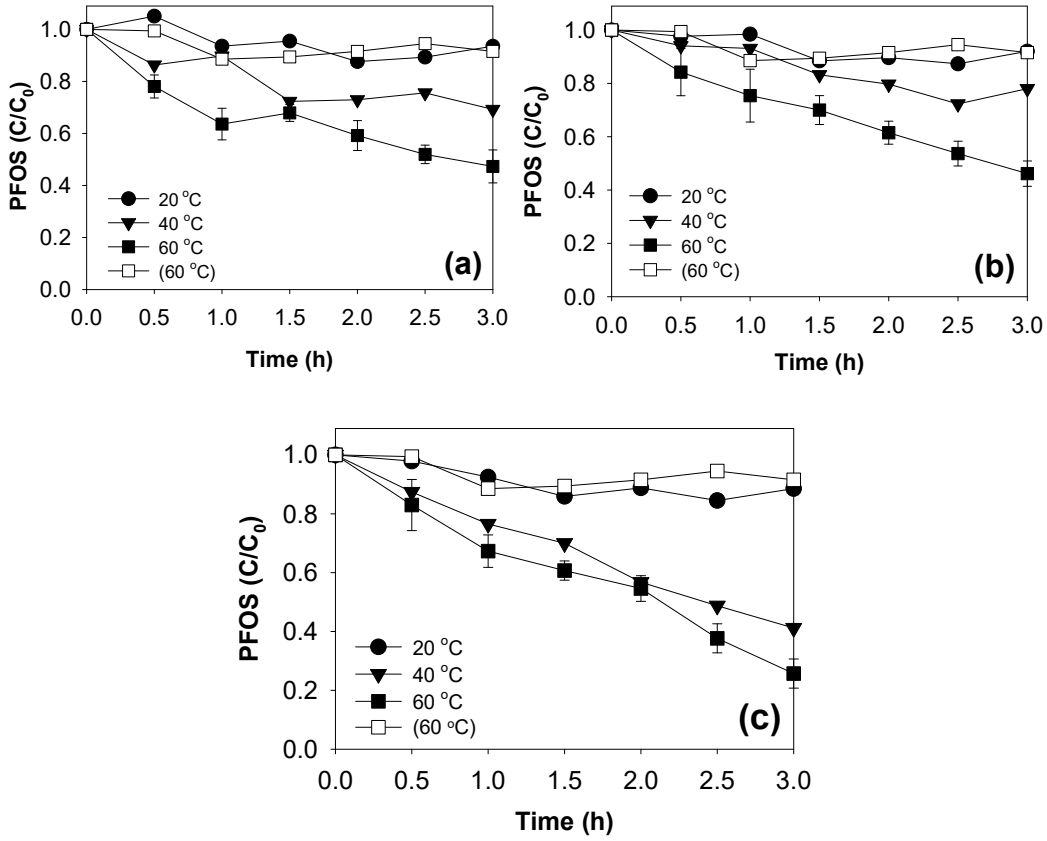

Figure 3-7: PFOS removal by ZVI conjugated with oxidant (a) PS, (b) PMS, and (c) HP at different temperatures (10 mg/L PFOS; 0.5 g/L ZVI; 0.3 M PS, 0.3 M PMS or 1.5 M HP; initial pH 3; 20, 40 or 60 °C). (60 °C) indicates the effect of ZVI alone (no oxidant) on the removal of PFOS at 60 °C. The error bars are the standard deviation of triplicate results.

Oxidant dose was varied in the presence of ZVI to investigate its effect on PFOS removal. Concentration was varied in two levels, namely high and low (by a factor of ten), as shown in Fig. 3-8.

The high dose was used as the standard condition for previous experiments. Higher concentration of PS, PMS, and HP resulted in faster removal kinetics of PFOS, but the increase was not significant considering a 10-fold concentration difference.

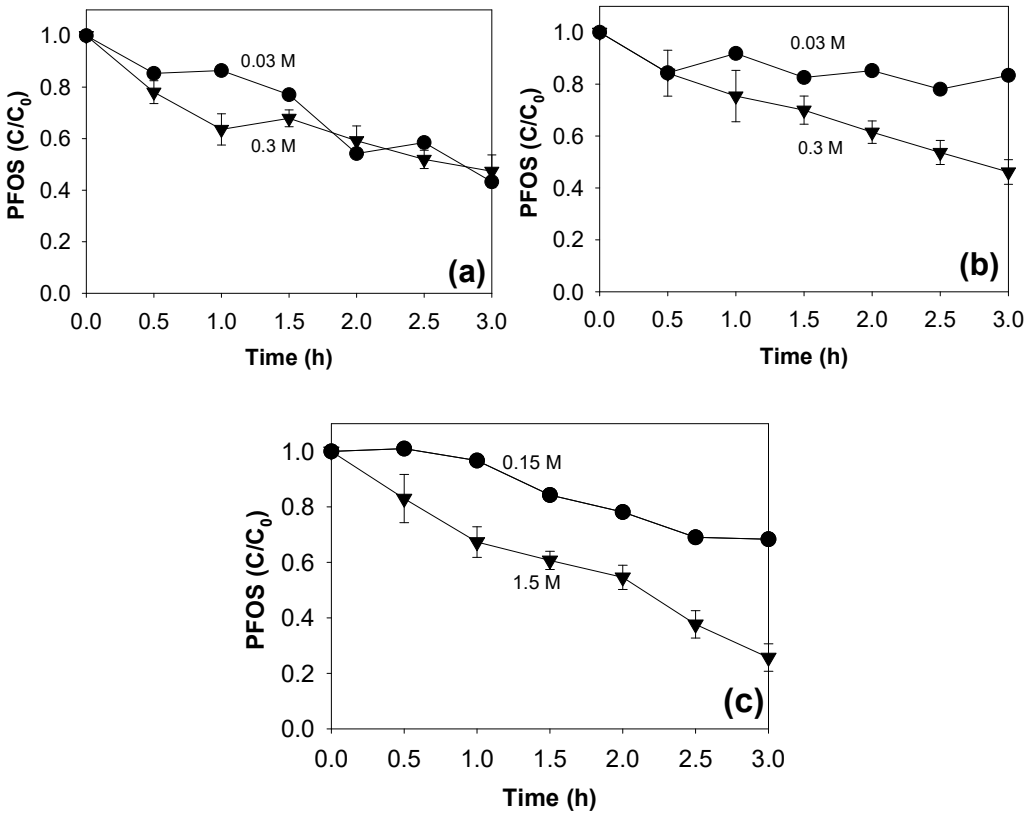

Figure 3-8: PFOS removal by ZVI conjugated with oxidant (a) PS, (b) PMS, and (c) HP at different concentrations (10 mg/L PFOS; 0.5 g/L ZVI; 0.03 or 0.3 M PS, 0.03 or 0.3 M PMS, 0.15 or 1.5 M HP; initial pH 3; 60 °C).

As shown in Fig. 3-9, initial pH was adjusted at 3 (acidic), 7 (neutral), and 9 (basic) without using any buffer species which also react with radicals and cause analytical inhibition.

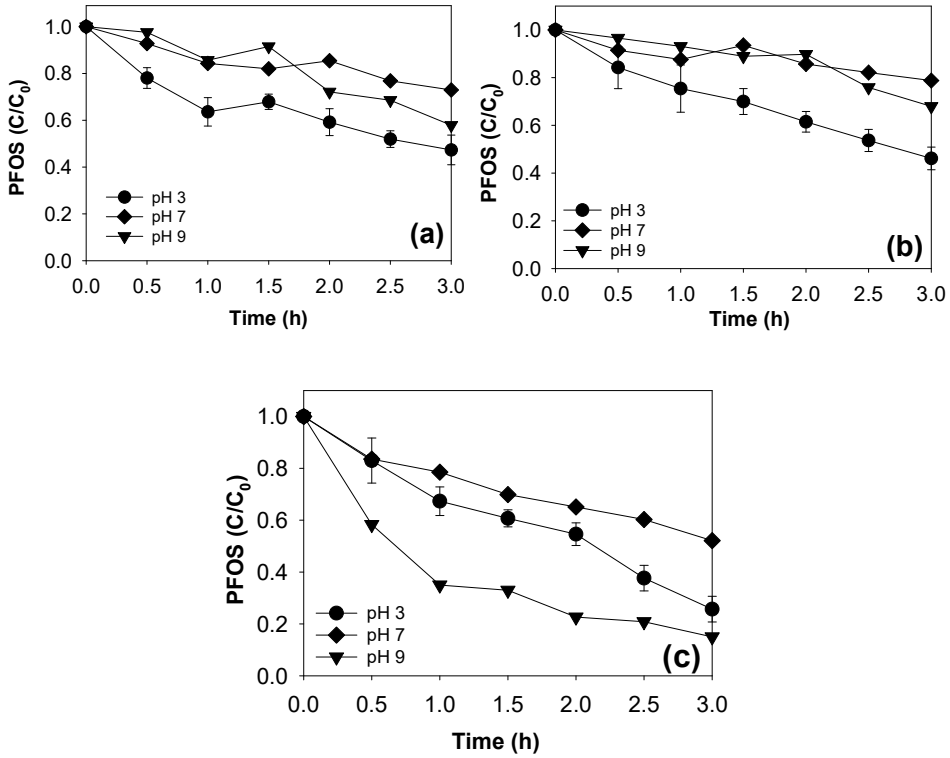

Figure 3-9: PFOS removal by ZVI conjugated with oxidant (a) PS, (b) PMS, and (c) HP at different initial pH conditions (10 mg/L PFOS; 0.5 g/L ZVI; 0.3 M PS, 0.3 M PMS or 1.5 M HP; initial pH 3, 7 or 9; 60 °C).

PS and PMS in the presence of ZVI showed slightly better PFOS removal at acidic pH (Wang and Wang, 2018). PFOS removal by HP in the presence of ZVI greatly changed upon pH. Basic pH was beneficial to PFOS removal. Previous studies proposed that HP can be activated by Fe ions at basic pH to generate O2•- and hydroperoxyl radicals as strong reducing species (Hayyan et al., 2016; da Silva-Rackov et al., 2016). Generation of

specific radicals and their reactivity are known to be dependent on reaction pH (Nfodzo et al., 2012). Reaction pH also affects the chemistry of PFOS interaction with compounds (Zhang et al., 2018; Cheng et al., 2009). Lastly, pH greatly controls the release of Fe^{2+} ions from ZVI, speciation of iron, and surface composition and chemistry of ZVI, which all influence the overall reaction kinetics in a complex way (Ling et al., 2018).

3.3.6 Discussion on Removal Mechanism.

Considerable removal of PFOS was observed in most of the cases tested. Since the integrated system uses solid ZVI, two possible mechanisms are considered to explain the observed PFOS removal: physical removal of PFOS to ZVI-associated species and/or chemical decomposition of PFOS by oxidation and/or reduction. In all the cases including the case showing the highest PFOS removal in Fig. 3-7c for ZVI+HP at 60 °C, increase in fluoride ion levels in the aqueous phase was not noticeable over the reaction time. Fluoride potentially on ZVI surface was also extracted, but fluoride concentration was negligible. Although formation of hydrofluoric acid could potentially occur under the final pH range of 1.5-4.5, we stop further investigating fluorine species assuming no significant defluorination (no reaction byproducts were observed later). Thus, the PFOS removal can be explained by its adsorption to and complexation with Fe species such as ZVI, Fe oxides and dissolved Fe ions and oxidation to unidentifiable intermediates (i.e., no significant defluorination of PFOS). To clarify the mechanism between adsorption and oxidation, F19-NMR and LC-MS analyses of the samples were introduced. NMR did not detect any significant alteration of PFOS structure. Further, MRM mode was employed in MS/MS analysis to search for targeted reaction intermediates, particularly shorter-chain PFAS that were expected to be produced during the decomposition of PFOS. However, expected intermediates were not detected.

The results possibly propose adsorption as a major mechanism to explain the observed PFOS removal and raise many possible complex scenarios occurring in the ZVI-based integrated system. Previous studies reported that adsorption of PFAS onto ZVI surface was considerably high (Zhang et al., 2018; Park et al., 2018; Lawal and Choi, 2018). Although ZVI itself does not show significant adsorption of PFOS, corrosion layers of iron oxides and iron hydroxides formed as a result of ZVI oxidation might adsorb PFOS better (Kim et al., 2018). For example, adsorption of PFOS onto RNIP and ZVI alone with high surface area of more than 30 m^2/g was negligible (Fig. 3-5a). As also shown in Fig. 3-7, ZVI combined with any oxidants at 60 °C showed higher PFOS removal while ZVI alone at 60 °C showed slight or negligible PFOS removal. This strongly suggests ZVI, when fast oxidized by added oxidants, can remove PFOS better.

The results shown in Fig. 3-8 might also support the removal mechanism. In spite of a 10 times higher concentration of oxidants where much more radicals were expected to be generated, PFOS removal was only slightly improved. It should also be noted that excess oxidant is capable of scavenging generated radicals (Nfodzo and Choi, 2011). The PFOS removal cannot be explained by the radical generation mechanism. Rather, higher oxidant dose may facilitate corrosion of ZVI and thus cause fast adsorption of PFOS to newly formed oxide and hydroxide layers with the chemical affinity for PFOS (Choi et al., 2009b). Significant amounts of PFOS were removed in all the cases involving ZVI and oxidant. Based on the formation of Fe oxides around core ZVI particle due to its corrosion as observed through XRD analysis of spent ZVI and reported elsewhere (Choi et al., 2009b), the effect of solid Fe_2O_3 (Fe^{3+}) and FeO (Fe^{2+}) on the removal (presumably adsorption) of PFOS under different pH conditions was revealed in Fig. 3-10. Acidic pH compared to basic pH and Fe_2O_3 compared to FeO seemed more beneficial to PFOS removal.

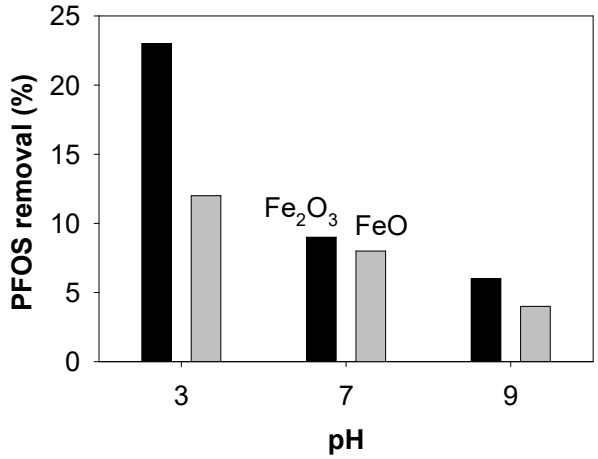

Figure 3-10: PFOS removal by adsorption to solid Fe_2O_3 and FeO particles under different initial pH conditions (10 mg/L PFOS; 0.5 g/L as Fe; initial pH 3, 7 or 9; 60 °C).

However, in the experiment conducted under pH 3 (e.g., in Figs. 3-8 and 3-9), Fe species were soluble under the pH condition and thus a small amount of solid ZVI and/or Fe oxides was available as potential PFOS adsorption sites.

To further explain the high PFOS removal even in the case, PFOS removal was attempted with dissolved Fe^{3+} and Fe^{2+} ions, as shown in Fig. 3-11, where Fe ions have potential to bind PFOS to make a complex. Apparently, higher Fe doses and Fe^{3+} ions compared to Fe^{2+} (as the finding in Fig. 3-11) exhibited better PFOS removal. At concentration of 2 g/L of Fe ions under acidic conditions, PFOS removal by Fe^{3+} was at 20% while that by Fe^{2+} was at 9%. Fe^{3+} showed better capability to make complex with PFOS. Similar results were reported by a study on the complexation of PFOS with different valence states of Fe (Park et al., 2018). Such Fe-PFOS complexes pose a challenge for prediction and quantification through MS analysis.

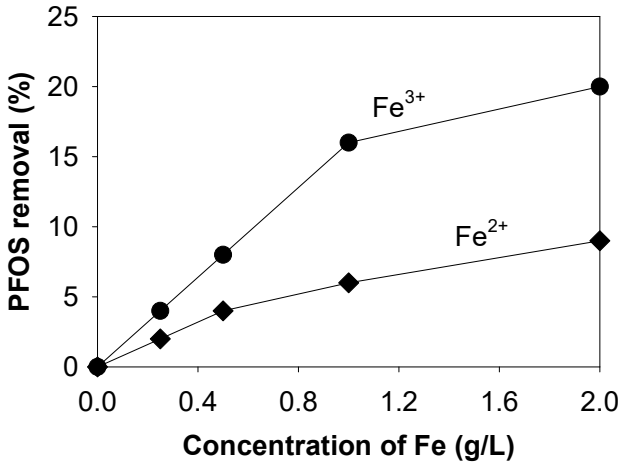

Figure 3-11: PFOS removal by complexation with dissolved Fe^{3+} and Fe^{2+} ions under different Fe doses (10 mg/L PFOS; 0.25-2 g/L as Fe; initial pH 3; 60 °C).

The removal of PFOS through either adsorption or complexation (i.e., no chemical decomposition) posed a question about the PFAS treatment potential of the proposed strategy combining oxidation and reduction. We briefly checked if the complexity of the removal mechanism is only for PFOS or it is consistent to other PFAS. PFOA, with a very similar structure to PFOS (both are C8 PFAS), was quickly examined. Figure 3-12 shows removal of PFOA and PFOS in comparison by using ZVI+PS system. PFOA removal was comparable to PFOS removal. PFOS removal was faster during the initial phase and then removal of both PFOA and PFOS later was very similar.

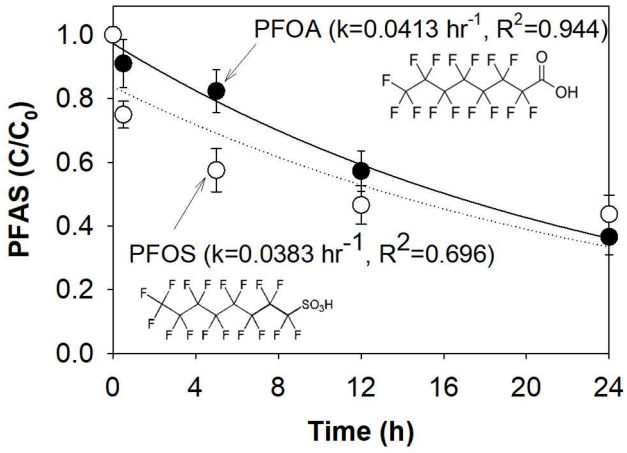

Figure 3-12: Removal of PFOS (empty circle) and PFOA (solid circle) by ZVI conjugated with PS (10 mg/L PFOA or PFOS; 0.5 g/L ZVI; 0.3 M PS; initial pH 3; 60 °C). First order reaction model lines are also shown for PFOA (solid line) and PFOS (dotted line). Insets are the chemical structure of PFOS and PFOA with multiple C−F bonds.

Compared to no identifiable intermediates from PFOS, targeted MS/MS analysis indicated formation of several reaction intermediates from PFOA, i.e., shorter-chain PFAS such as PFHpA (C7), PFHxA (C6), PFPeA (C5), and PFBA (C4), as shown in Fig. 3-13. The mechanism of PFOA decomposition seems to be a progressive removal of CF_2 moieties to form the shorter-chain PFAS (Bruton and Sedlak, 2018; Hori et al., 2005).

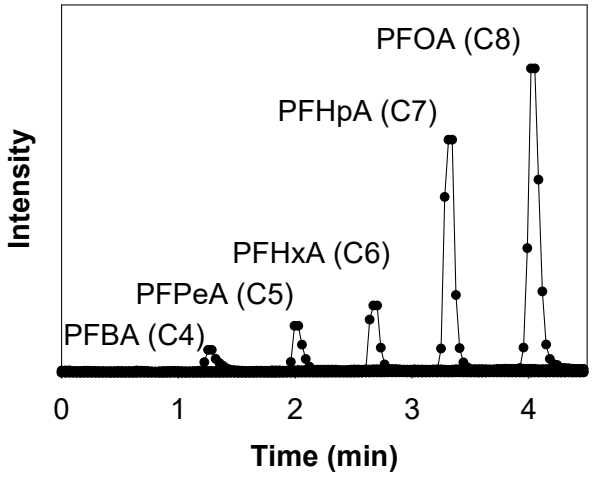

Figure 3-13: Identification of reaction intermediates formed during the decomposition of PFOA by ZVI conjugated with PS. Confirmation of the reaction intermediates was undertaken using targeted analysis based on our expectation, while many other intermediates were also formed.

Now, the observed decomposition of PFOA by the ZVI-based integrated system raises more questions that should be investigated in near future. PS itself is capable of decomposing PFOA in literature but it requires high temperatures (Bruton and Sedlak, 2018). In this current study, PS is activated by Fe ions released from ZVI, along with heat activation of PS. The proposed ZVI-PS system at high temperatures might generate reactive species more effectively than only PS at high temperatures, resulting in potential reduction of temperature requirements for PFAS decomposition. Nonetheless, the ZVI-based integrated system combining oxidation and reduction works for the chemical decomposition of PFOA (and presumably other PFAS, in particular, carboxylic PFAS), but not for PFOS. Previous studies also reported a greater persistence of PFOS when compared to PFOA presumably due to the carboxylic functional group in PFOA being more

vulnerable to chemical reaction than the sulfonic functional group in PFOS (Bruton and Sedlak, 2018; Park et al., 2016; Mitchell et al., 2014).

The strategy of using ZVI conjugated with oxidants was initially thought to be less dependent on the functional groups, considering both molecules possess overall very similar molecular structures. Interestingly, one (PFOA) was decomposed while the other (PFOS) was not decomposed. It should be investigated that the finding is applicable to other carboxylic PFAS in comparison to other sulfonate PFAS. Many other possibilities are also under consideration, including formation of insoluble (thus undetectable) PFOS dimer as a result of PFOS decomposition. Along with elucidating the decomposition mechanism of PFOA and (if any) PFOS, many other PFAS with different chain lengths and functional groups should be further examined with the ZVI-based system to answer the questions.

Combining advanced oxidation with chemical reduction by exploiting various oxidizing and reducing reactive species generated in the proposed system turned out to be not so effective for PFOS decomposition but to work for PFOA decomposition. Defluorination should be proceeded by other chemical or photochemical processes somehow for the decomposition of PFOS. Lastly, if proven successful in removing PFAS (at least carboxylic PFAS) via adsorption, complexation, and/or decomposition, the concept of this study can be directly applied with reactive barrier concept incorporating ZVI and oxidant injection to treat groundwater or heterogeneous media including soil and sediment as demonstrated for other halogenated chemicals (Choi et al., 2015). These all also need to be investigated in the near future.

3.4 Conclusions

This feasibility study examined if the ZVI-based integrated system exhibiting the capabilities of advanced oxidation, reductive dehalogenation, and possibly adsorption can

remove and decompose PFOS under various conditions. In most of the experimental cases, a substantial amount of PFOS was removed. However, building up of identifiable expected intermediates and fluoride ions in water was negligible. The observed PFOS removal could be ascribed to presumably its adsorption to and complexation with Fe species such as Fe oxides and dissolved Fe ions originated from ZVI particles. The brief comparison between PFOS and PFOA raised more questions because PFOA (and presumably other PFAS) can be decomposed by the treatment system, generating obvious reaction intermediates such as shorter-chain PFAS. The results indicated that PFOS, unlike PFOA, seems much more stable even in the presence of the strong reactive species produced under the tested experimental conditions. Many possible complex scenarios occurring in the integrated system were discussed. In-depth studies are needed in near future to narrow down the complex scenarios. Additional PFAS with different structures should be examined to obtain insight into their chemical reactivity with the integrated system. Finally, modifications of the treatment system are highly needed to further enhance the observed decomposition kinetic of PFOA and tackle the most challenging PFOS, such as use of other oxidants (e.g., ferrate) and surface-modified ZVI, addition of catalysts, intermittent addition of oxidants, and prevention of initial oxidation to facilitate reduction.

3.5 References

Appleman, T. D., Higgins, C. P., Quinones, O., Vanderford, B. J., Kolstad, C., Zeigler-Holady, J. C., and Dickenson, E. R. V. (2014). Treatment of poly- and perfluoroalkyl substances in U.S. full-scale water treatment systems. Water Res. 51, 246-255.

Arvaniti, O. S., Hwang, Y., Andersen, H. R., Stasinakis, A. S., Thomaidis, N. S., and Aloupi, M. (2015). Reductive degradation of perfluorinated compounds in water using Mg-aminoclay coated nanoscale zero valent iron. Chem. Eng. J. 262, 133-139.

Bennedsen, L. R. (2014). Chapter 2 - In situ chemical oxidation. The mechanisms and applications of chemical oxidants for remediation purposes. In E.G. Sogaard, Ed., Chemistry of advanced environmental purification processes of water - Fundamentals and applications. Amsterdam, Netherlands: Elsevier, p 13.

Blotevogel, J., Giraud, R. J., and Borch, T. (2018). Reductive defluorination of perfluorooctanoic acid by zero-valent iron and zinc: A DFT-based kinetic model. Chem. Eng. J. 335, 248-254.

Brillas, E., Mur, E., Sauleda, R., Sànchez, L., Peral, J., Domènech, X., and Casado, J. (1998). Aniline mineralization by AOP's: anodic oxidation, photocatalysis, electro-Fenton and photoelectro-Fenton processes. Appl. Catal. B: Environ. 16(1), 31-42.

Bruton, T. A., and Sedlak, D. L. (2018). Treatment of perfluoroalkyl acids by heat-activated persulfate under conditions representative of in situ chemical oxidation. Chemosphere 206, 457-464.

Bruton, T. A., and Sedlak D. L. (2017). Treatment of aqueous film-forming foam by heat-activated persulfate under conditions representative of in situ chemical oxidation. Environ. Sci. Technol. 51(23), 13878-13885.

Cheng, J., Psillakis, E., Hoffmann, M. R., and Colussi, A. J. (2009). Acid dissociation versus molecular association of perfluoroalkyl oxoacids: environmental implications. J. Phys. Chem. A 113(29), 8152.

Choi, H., Lawal, W., Al-Abed, S. R. (2015). Desorption, partitioning, and dechlorination characteristics of PCBs in Waukegan Harbor sediment under remediation with reactive activated carbon. J. Haz. Mat. 287,118-125.

Choi, H., Al-Abed, S. R., Dionysiou, D. D., Stathatos, E., and Lianos, P. (2010). Chapter 8 TiO2-based advanced oxidation nanotechnologies for water purification and reuse. In I.C. Escobar and A.I. Schafer, Eds., Sustainability Science and Engineering, Vol. 2. Elsevier, p. 229.

Choi, H., Agarwal, S., Al-Abed, S. R. (2009a) Adsorption and simultaneous dechlorination of PCBs by GAC impregnated with ZVI/Pd bimetallic particles: Mechanistic aspects and reactive capping barrier concept. Environ. Sci. Technol. 43, 488-493.

Choi, H., Al-Abed, S. R., Agarwal, S. (2009b). Effects of ageing and oxidation of palladized iron embedded in activated carbon on the dechlorination of 2-chlorobiphenyl. Environ. Sci. Technol. 43(11), 4137-4142.

Choi, H., Al-Abed, S. R., Agarwal, S., Dionysiou, and Dionysios, D. (2008). Synthesis of Reactive Nano-Fe/Pd Bimetallic System-Impregnated Activated Carbon for the Simultaneous Adsorption and Dechlorination of PCBs. Chem. Mater. 20(11), 3649-3655.

Da Silva-Rackov, C. K. O., Lawal, W. A., Nfodzo, P. A., Vianna, M. M. G. R., do Nascimento, Claudio A. O., and Choi, H. (2016). Degradation of PFOA by hydrogen peroxide and persulfate activated by iron-modified diatomite. Appl. Catal. B_Environ. 192, 253-259.

Dasu, K., Lee, L. S., Turco, R. F., Niles, L. F. (2013). Aerobic biodegradation of 8:2 fluorotelomer stearate monoester and 8:2 fluorotelomer citrate triester in forest soil. Chemosphere 91 (3), 399-405.

Dillert, R., Bahnemann, D., and Hidaka, H. (2007). Light-induced degradation of perfluorocarboxylic acids in the presence of titanium dioxide. Chemosphere 67(4), 785-792.

Eriksson, U., Haglund, P., Karrman, A. (2017). Contribution of precursor compounds to the release of per- and polyfluoroalkyl substances (PFASs) from waste water treatment plants (WWTPs), J. Environ. Sci. 61, 80-90.

Fu, F., Dionysiou, D. D., and Liu, H. (2014). The use of zero-valent iron for groundwater remediation and wastewater treatment: A review. J. Haz. Mater. 267, 194-205.

Hayyan, M., Hashim, M. A., and AlNashef, I. M., (2016). Superoxide ion: generation and chemical implications. Chemical Rev. 116, 3029-3085.

Hori, H., Yamamoto, A., Koike, K., Kutsuna, S., Osaka, I., and Arakawa, R. (2007). Photochemical decomposition of environmentally persistent short-chain perfluorocarboxylic acids in water mediated by iron (2+)/(2+I) redox reactions. Chemosphere 68(3), 572-578.

Hori, H., Nagaoka, Y., Yamamoto, A., Sano, T., Yamashita, N., Taniyasu, S., Kutsuna, S., Osaka, I., and Arakawa, R. (2006). Efficient decomposition of environmentally persistent perfluorooctanesulfonate and related fluorochemicals using zerovalent iron in subcritical water. Environ. Sci. Technol. 40(3), 1049-1054.

Hori, H., Yamamoto, A., Hayakawa, E., Taniyasu, S., Yamashita, N., Kutsuna, S., Kiatagawa, H., and Arakawa, R. (2005). Efficient decomposition of environmentally persistent perfluorocarboxylic acids by use of persulfate as a photochemical oxidant. Environ. Sci. Technol. 39(7), 2383-2388.

Houtz, E. F., Higgins, C. P., Field, J. A., and Sedlak, D. L. (2013). Persistence of perfluoroalkyl acid precursors in AFFF-impacted groundwater and soil. Environ. Sci. Technol. 47(15), 8187-8195.

Kim, C., Ahn, J., Kim, T. Y., Shin, W. S., and Hwang, I. (2018). Activation of Persulfate by Nanosized Zero-Valent Iron (NZVI): Mechanisms and Transformation Products of NZVI. Environ. Sci. Technol. 52(6), 3625-3633.

Kissa, E. (1994). Fluorinated surfactants. Dekker, NY: Marcel Dekker Inc.

Lawal, W. A., Choi, H. (2018). Feasibility study on the removal of perfluorooctanoic acid by using palladium-doped nanoscale zerovalent iron. J. Env. Eng. 144(11): 04018115.

Lee, Y., Lo, S., Chiueh, P., Liou, Y., and Chen, M. (2010). Microwave-hydrothermal decomposition of perfluorooctanoic acid in water by iron-activated persulfate oxidation. Water Res. 44(3), 886-892.

Lee, Y., Lo, S., Chiueh, P., and Chang, D. (2009). Efficient decomposition of perfluorocarboxylic acids in aqueous solution using microwave-induced persulfate. Water Res. 43(11), 2811-2816.

Lefevre, E., Bossa, N., Wiesner, M. R., and Gunsch, C. K. (2016). A review of the environmental implications of in situ remediation by nanoscale zero valent iron (nZVI): Behavior, transport and impacts on microbial communities. Sci. Total Environ. 565, 889-901.

Ling, R., Chen, J. P., Shao, J., and Reinhard, M. (2018). Degradation of organic compounds during the corrosion of ZVI by hydrogen peroxide at neutral pH: Kinetics, mechanisms and effect of corrosion promoting and inhibiting ions. Wat. Res. 134, 44-53.

Liu, Y., Choi, H. Dionysiou, D. D., Lowry, G. V. (2006). Trichloroethene hydrodechlorination in water by highly disordered monometallic nanoiron. Chem. Mater. 17(21), 5315-5322.

Lyu, X., Li, W., Lam, P. K. S., Yu, H. (2015) Insights into perfluorooctane sulfonate photodegradation in a catalyst-free aqueous solution. Sci. Rep. 5 (9353), 1-6.

Merino, N., Qu, Y., Deeb, R. A., Hawley, E. L., Hoffmann, M. R., and Mahendra, S. (2016). Degradation and removal methods for perfluoroalkyl and polyfluoroalkyl substances in water. Environ. Eng. Sci. 33(9), 615-649.

Mitchell, A. M., Ahmad, M., Teel, A. L., and Watts, R. J. (2014). Degradation of perfluorooctanoic acid by reactive species generated through catalyzed H2O2 propagation reactions. Environ. Sci. Technol. Lett. 1, 117-121.

Moriwaki, H., Takagi, Y., Tanaka, M., Tsuruho, K., Okitsu, K., and Maeda, Y. (2005). Sonochemical decomposition of perfluorooctane sulfonate and perfluorooctanoic acid. Environ. Sci. Technol. 39(9), 3388-3392.

Nfodzo, P., Hu, Q., Choi, H. (2012). Impacts of pH-dependent metal speciation on the decomposition of triclosan by sulfate radicals. Water Sci. Technol.: Water Supply 12(6) 837-843.

Nfodzo, P., Choi, H. (2011). Triclosan decomposition by sulfate radicals: effects of oxidant and metal doses. Chem. Eng. J. 174 629-634.

Oh, S., Kang, S., and Chiu, P. C. (2010). Degradation of 2,4-dinitrotoluene by persulfate activated with zero-valent iron. Sci. Total Environ. 408(16), 3464-3468.

Ollis, D. F., Pelizzetti, E., and Serpone, N. (1991). Photocatalyzed destruction of water contaminants. Environ. Sci. Technol. 25(9), 1522-1529.

Panchangam, S. C., Lin, A. Y., Lin, C., and Tsai, J. (2009). Sonication-assisted photocatalytic decomposition of perfluorooctanoic acid. Chemosphere 75(5), 654-660.

Park, S., Zenobio, J. E., and Lee, L. S. (2018). Perfluorooctane sulfonate (PFOS) removal with Pd0/nFe0 nanoparticles: Adsorption or aqueous Fe-complexation, not transformation? J. Haz. Mater. 342, 20-28.

Park, S., Lee, L. S., Medina, V. F., Zull, A., and Waisner, S. (2016). Heat-activated persulfate oxidation of PFOA, 6:2 fluorotelomer sulfonate, and PFOS under conditions suitable for in-situ groundwater remediation. Chemosphere 145, 376-383.

Park, H., Vecitis, C. D., Cheng, J., Dalleska, N.F., Mader, B. T., Hoffmann, M. R. (2011). Reductive degradation of perfluoroalkyl compounds with aquated electrons generated from iodide photolysis at 254 nm. Photochem. Photobiol. Sci. 10, 1945-1953.

Rayne, S., and Forest, K. (2009). Perfluoroalkyl sulfonic and carboxylic acids: A critical review of physicochemical properties, levels and patterns in waters and wastewaters, and treatment methods. J. Environ. Sci. Health, Part A 44(12), 1145-1199.

Rodriguez, S., Vasquez, L., Romero, A., Santos, A., and Santos, A. (2014). Dye oxidation in aqueous phase by using zero-valent iron as persulfate activator: Kinetic model and effects of particle size. Ind. Eng. Chem. Res. 101(31), 86-92.

Trojanowicz, M., Bojanowska-Czajaka, A., Bartosiewicz, I., Kulisa, K. (2018). Advanced oxidation/reduction processes for aqueous perfluorooctanoate (PFOA) and perfuorooctanesulfonate (PFOS) - A review of recent advances. Chem. Eng. J. 336, 170-199.

United States Environmental Protection Agency (USEPA). (2018). US Environmental Protection Agency, National Priorities: PER-AND POLYFLUOROALKYL SUBSTANCES (EPA-G2018-ORD-A1). Washington, DC: USEPA. Available at https://www.epa.gov/research-grants/national-priorities-and-polyfluoroalkyl-substances

United States Environmental Protection Agency (USEPA). (2016). US Environmental Protection Agency, Drinking Water Health Advisories for PFOA and PFOS (EPA-HQ-OW-2014-0138; FRL-9946-91-OW). Washington, DC: Office of the Federal Register, National Archives and Records Administration (NARA). Available at https://www.epa.gov/sites/production/files/2016-05/documents/2016-12361.pdf

Vecitis, C. D., Park, H., Cheng, J., Mader, B. T., and Hoffmann, M. R. (2009). Treatment technologies for aqueous perfluorooctanesulfonate (PFOS) and perfluorooctanoate (PFOA). Front. Environ. Sci. Eng. Chin., 3(2), 129-151.

Wang, J., and Wang, S. (2018). Activation of persulfate (PS) and peroxymonosulfate (PMS) and application for the degradation of emerging contaminants. Chem. Eng. J. 334, 1502-1517.

Watts, R. J., Yu, M., and Teel, A. L. (2017). Reactive oxygen species and associated reactivity of peroxymonosulfate activated by soluble iron species. J. of Contam. Hydrol. 205, 70-77.

Yang, S., Yang, X., Wang, P., Shan, L., Zhang, W., Shao, X., and Niu, R. (2010). Degradation efficiencies of azo dye Acid Orange 7 by the interaction of heat, UV and anions with common oxidants: Persulfate, peroxymonosulfate and hydrogen peroxide. J. Hazard. Mater. 179(1), 552-558.

Zhang, W., Gao, H., He, J., Yang, P., Wang, D., Ma, T., Xia, H., and Xu, X. (2017). Removal of norfloxacin using coupled synthesized nanoscale zero-valent iron (nZVI) with

H2O2 system: Optimization of operating conditions and degradation pathway. Sep. Purif. Technol. 172, 158-167.

Zhang, Y., Zhi, Y., Liu, J., and Ghoshal, S. (2018). Sorption of perfluoroalkyl acids to fresh and aged nanoscale zerovalent iron particles. Environ. Sci. Technol. 52(11), 6300-6308.

Zhao, J., Zhang, Y., Quan, X., and Chen, S. (2010). Enhanced oxidation of 4-chlorophenol using sulfate radicals generated from zero-valent iron and peroxydisulfate at ambient temperature. Sep. Purif. Technol. 71(3), 302-307.

Chapter 4

Silver-activated persulfate

4.1 Introduction

Due to their unique properties such as repelling both water and oil, per- and polyfluoroalkyl substances (PFAS) have been widely used in many industrial and military products (e.g., water and stain repellent, non-stick cookware, aqueous film-forming foam) (Kissa, 1994). However, PFAS, also referred as “forever chemicals”, have gained recent notoriety due to concerns over health and environmental impacts (Macheka-Tendenguwo et al., 2018; Domingo and Nadal 2017; Crawford et al., 2017). The United States Environmental Protection Agency has set an advisory limit of 70 ng/L for perfluorooctanoic acid (PFOA) and perfluorooctanesulfonic acid (PFOS), the two most prevalent PFAS (USEPA, 2016).

PFAS vary in carbon chain lengths and functional groups (Buck et al., 2017). Once released to the environment, some of them undergo bio-chemical transformations to more oxidized forms which ultimately become more recalcitrant, such as perfluorocarboxylic acids (PFCA or carboxylic PFAS) such as PFOA and perfluorosulfonic acids (PFSA or sulfonic PFAS) such as PFOS (Shaw et al., 2019). They are not (or rarely) decomposed in either natural environments or treatment facilities due to the chemical inertness of the extraordinarily strong, highly-polarized C−F bonds and the chemical stability of the carbon chain with a functional group (e.g., carboxylic acid or sulfonic acid) at one extremity, while significantly contaminating our water resources. Thus, conventional chemical oxidation processes employing common oxidants alone such as hydrogen peroxide (HP, H_2O_2), persulfate (PS, $S_2O_8^{2-}$), and peroxymonosulfate (PMS, HSO_5^-) are known to be not effective to decompose PFAS under ambient conditions (Merino et al., 2016).

Attention has been given to advanced oxidation technologies (AOTs), which utilize strong transient oxidizing species such as hydroxyl radicals (HRs, $^{\bullet}OH$) and sulfate radicals (SRs, $SO_4^{\bullet-}$) (Choi et al., 2010). Among many AOTs, the radicals can be practically generated under ambient conditions via activation of HP with iron (Fe), commonly known as the Fenton reaction (Nfodzo and Choi, 2011; Anipsitakis et al., 2004). However, the Fenton reaction proven to work for a variety of persistent organic chemicals has not yet been reported to be effective for perfluoroalkyl substances and PFAS in more oxidized forms, such as PFOA and PFOS (Merino et al., 2016; Vecitis et al., 2009).

In fact, research studies involving AOTs introduce additional working mechanisms such as photolysis, thermolysis, and sonolysis along with HRs and SRs mechanisms to decompose PFAS more effectively. They include H_2O_2/UV photo-Fenton, TiO_2/UV photocatalysis, and sonochemical processes for HRs generation as well as $S_2O_8^{2-}$/UV, HSO_5^-/UV, and $S_2O_8^{2-}$/microwave for SRs generation (Merino et al., 2016; Vecitis et al., 2009; Rayne and Forest, 2009). Especially, PS, one of the most widely used oxidants in in-situ chemical oxidation processes, was reported to require high temperatures at around 60−90 °C to decompose exclusively PFCA such as PFOA, but PFSA such as PFOS were not decomposed even under the conditions (Bruton and Sedlak, 2018 and 2017; Park et al. 2016). In a recent review article, Yang et al. (2020) well compared activation methods for PS by ultraviolet, ultrasound, microwave, and/or heat. In spite of their effectiveness, these technologies commonly require extreme conditions, leading to higher costs and lowering the potential for practical applicability.

As a result, it is imperative to decompose PFAS under ambient conditions by using practical technologies for full scale applications. We propose to activate PS simply with transition metals such as silver (Ag) without introducing any energy-intensive tools. Herein, we, for the first time, communicate the potential of the modified Fenton system, i.e.,

homogeneous PS conjugated with Ag^+, to decompose PFAS at 20 ˚C, particularly perfluorinated ones. Combinations of common oxidants and transition metals were evaluated to decompose 4 selected PFAS, while fluoride ion release and reaction byproduct formation were traced. Results from this study may provide insightful information on ways to tackle the ever-challenging issue of PFAS decomposition.

4.2 Methods

4.2.1 Chemicals and Reagents

Perfluorononanoic acid (PFNA, $C_9F_{17}O_2H$, CAS 357-95-1), PFOA ($C_8F_{15}O_2H$, CAS 335-67-1), perfluorheptanoic acid (PFHpA, CAS 357-85-9), PFOS ($C_8F_{17}SO_3K$, CAS 2795-39-3), ferrous sulfate ($FeSO_4{\cdot}7H_2O$), cobalt sulfate ($CoSO_4.7H_2O$), and silver sulfate (Ag_2SO_4) were purchased from Sigma-Aldrich (St. Louis, MO). Internal standards for all parent and byproduct PFAS were purchased from Wellington Laboratories Inc. (Ontario, Canada). Acetonitrile (ACN, C_2H_3N), potassium iodide (KI), sodium bicarbonate ($NaHCO_3$), tert-butyl alcohol (TBA, $(CH_3)_3COH$), methanol (CH_4O), and formic acid (CH_2O_2) were acquired from Fisher Chemical (Fair Lawn, NJ). Large molecule separation (LMS, 200 mg, 3 mL) cartridge for solid phase extraction was purchased from Agilent Technologies (Santa Clara, CA). All solutions and sample preparations were done in ultrapure water. All chemicals were used as received.

4.2.2 Batch Experiment

Reactions were carried over 48 hr in 20 mL sealed polypropylene reaction vials containing a final volume of 20 mL (no head space available) with 10 mg/L of each PFAS. Concentration of PS was fixed at 0.15 M as a standard while ranging up to 0.6 M; concentration of transition metals such as Ag^+, Fe^{2+}, and cobalt (Co^{2+}) was fixed at 0.6 mM

while ranging up to 1.2 mM; and reaction temperature was fixed at 20 °C while ranging up to 80 °C. Although there might be a threshold concentration of metals required to activate oxidants and an optimum ratio of metal to oxidant dose due to scavenging effects, relatively high concentrations of metals were used to quickly evaluate if PFAS is decomposed under the reaction conditions, following values reported elsewhere (Nfodzo and Choi, 2011; Anipsitakis and Dionysiou, 2004). Radical scavenger tests were conducted to identify the role of radical species, using 0.3 M of TBA or methanol. TBA is known to react significantly faster with HRs than SRs while methanol scavenges both radicals at similar rates (Anipsitakis and Dionysiou, 2004; Buxton et al., 1988; Neta et al., 1988). The final volume was adjusted to attain the desired concentration of the reactants.

4.2.3 Sample Treatment and Chemical Analysis

Sample preparation and analysis were conducted as described in our previous study (Parenky et al., 2020). Basically, we followed the EPA Method 537 for general PFAS analytical procedures employing solid phase extraction and liquid chromatography/mass spectrometry (LC/MS) (USEPA, 2009). Briefly, samples of 0.2 mL were diluted in 1.8 mL of water. LMS cartridges were preconditioned using 3 mL of methanol and washed with 3 mL of water. Later, samples were extracted with methanol in a ratio of 1:1 and analyzed in a Shimadzu (Nakagyo-ku, Kyoto, Japan) Nexera LC equipped with a Shimadzu 8040 triple quadrupole MS. Flow rate was set at 0.3 mL/min with a binary gradient method. Mobile phase was 0.1% formic acid in water and in ACN. Separation was achieved by an Agilent Zorbax Eclipse Plus C18 RRHD column (50mm x 3mm x 1.8 µm particle size) and target analytes were eluted through a gradient method in which ACN was increased from 30% to 90% over 6 min, kept at 90% for 3 min, and then brought down to 30% in 3 min. Column temperature was set at 40 °C and sample injection was set at 10 µL. For quantification of

the target analytes such as PFNA, PFOA, PFHpA, and PFOS and expected byproducts such as short chain PFAS, multiple reaction monitoring scans were conducted in a negative electrospray ionization mode. Internal standards were used to develop calibration curves for parent PFAS and byproduct. Confirmation of expected reaction intermediates and byproduct was undertaken using targeted analysis. Monitored ion transitions of PFNA, PFOA, PFHpA, PFOS, perfluorohexanoic acid (PFHxA), perfluoropentanoic acid (PFPeA), and perfluorobutanoic acid (PFBA) were conducted, as described by Bruton and Sedlak (2017).

Aqueous fluoride ions detached from PFAS were measured by using a Hach (Loveland, CO) HQ 440D base combined with an Intellical ISE F121 electrode. Its detection limit was at 0.02 mg/L. Hach ionic strength adjuster (ISA) pack was diluted in 5mL of water. Samples of 0.5 mL were diluted with 0.5 mL ISA stock solution prior to analysis. Concentration of PS remaining in reaction solutions was traced using a spectrophotometric method (Liang et al. 2008). In brief, a stock solution containing 100 g/L of KI and 5 g/L of $NaHCO_3$ was prepared in water. Later, 0.5 mL of diluted sample was added to 4.5 mL of the stock solution and read at 400 nm in a Shimadzu 2550 UV-visible spectrophotometer.

4.3 Results and Discussion

It should be first noted that any disappearance of PFAS tested in this study is ascribed to their chemical decomposition (i.e., removal through any physical adsorption was not considered since all chemicals were homogeneously dissolved).

4.3.1 Heat-Activated PS:

To quickly confirm temperature requirement in the well-established heat-activated PS system, decomposition of PFOA was attempted by PS alone without transition metals at different temperatures of 20-80 °C, as shown in Fig. 4-1. PFOA was not decomposed at 20 °C while at least 40 °C was required to activate PS for PFOA decomposition. Under temperatures of 60 and 80 °C, PFOA decomposition kinetics were much faster, showing almost complete decomposition of PFOA within 6-8 h. Fluoride ions and short chain byproducts in water were also detected. However, PFOS was not decomposed even at 80 °C (data not shown). Previous studies have also reported similar temperature requirements at around 60-90 °C and pointed out SRs are responsible for PFOA decomposition while PFOS remains inert under such conditions (Yang et al., 2020; Bruton and Sedlak 2018 and 2017; Park et al., 2016). The results support the crucial role of heat to activate PS in order to generate SRs and increase reaction kinetics.

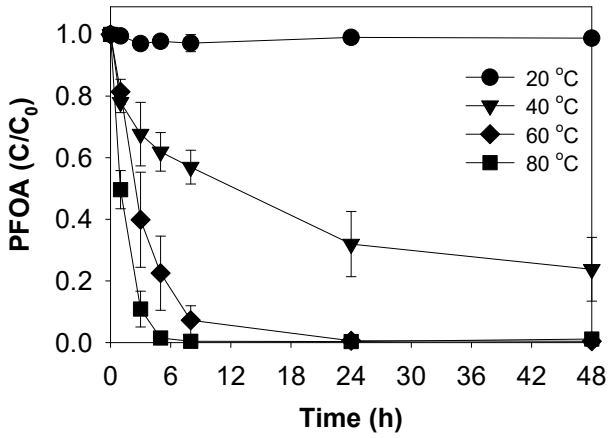

Figure 4-1: Decomposition of PFOA by PS alone at different temperatures (10 mg/L PFOA, no metal, 0.15 M PS, initial pH 4.5 to final pH around 1.5 (no pH control), temperature 20, 40, 60 or 80 °C). The error bars are the standard deviation of triplicated results.

4.3.2 Transition Metal-Activated PS:

Instead of heat to activate PS, we exploited transition metals including Fe2+, Co2+, and Ag^{+} for decomposition of PFOA at 20 °C, as shown in Fig. 4-2. PS/Fe^{2+} and PS/Co^{2+} were not effective at all while only PS/Ag+ showed noticeable decomposition of PFOA (please also note that experiments conducted with other oxidants such as HP and PMS conjugated with the metals did not show significant decomposition of PFOA, results not shown).

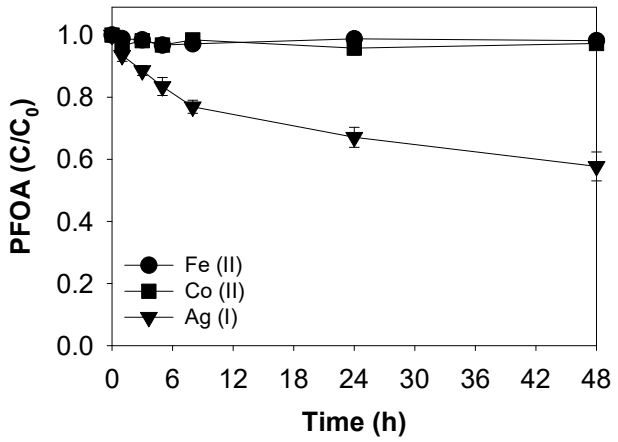

Figure 4-2: Decomposition of PFOA by PS conjugated with various transition metals (Fe^{2+}, Co^{2+} and Ag^{+}) at room temperature (10 mg/L PFOA, 0.6 mM metal, 0.15 M PS, initial pH 4.5 to final pH around 1.5 (no pH control), temperature 20 °C).

Activation of oxidants by transition metals to produce various radicals has been previously demonstrated (Wang and Wang, 2018; Nfodzo and Choi, 2011; Anipsitakis and Dionysiou, 2004). In general, Fe, Co, and Ag are the best activators for HP, PMS, and PS, respectively (Nfodzo and Choi, 2011; Anipsitakis and Dionysiou, 2004). However, the best combination of an oxidant and a metal has been also reported to depend on target chemicals and reaction conditions (Waclawek et al., 2017). PMS/Co^{2+} pair has been used to generate HRs and SRs for the decomposition of polyfluoroalkyl substances such as 6:2 fluorotelomer sulfonate, but not for perfluoroalkyl ones (Zhang et al., 2020). PS/Fe^{2+} pair has been the most studied due to the eco-friendly properties of Fe, and proven to be effective for decomposition of polyaromatic hydrocarbon such as anthracene through generation of HRs under neutral to basic pHs and/or SRs under acidic pHs (Peluffo et al., 2016). Anipsitakis and Dionysiou (2004) reported that 2, 4-dichlorophenol is decomposed

faster by PS conjugated with Ag^+ than other transition metals. Similarly, PS/Ag pair has been successful in decarboxylating levulinic acid in water (Gong and Lin, 2011).

Reaction between PS and Ag^+ was proposed by Anderson and Kochi (1970). Generation of SRs from PS and oxidation of Ag^+ to Ag^{2+} are shown in Eq. (16); transformation of the generated SRs to sulfate ions and oxidation of Ag^+ to Ag^{2+} are shown in Eq. (17); and decarboxylation of a carboxylic group and conversion of Ag^{2+} back to Ag+ are shown in Eq. (18). The Fenton-like reactions may also be applicable to certain oxidant/metal pairs. Both SRs and Ag^{2+} that is also highly reactive are believed to be responsible for the observed decomposition of PFOA in Fig. 2 via decarboxylation reaction, as also reported for other organic chemicals by Anipsitakis and Dionysiou (2004) and Gong and Lin (2011).

$$Ag^+ + S_2O_8^{2-} \rightarrow Ag^{2+} + SO_4^{\bullet -} + SO_4^{2-} \quad (16)$$

$$Ag^+ + SO_4^{\bullet -} \rightarrow Ag^{2+} + SO_4^{2-} \quad (17)$$

$$Ag^{2+} + RCO_2H \rightarrow Ag^+ + RCO_2^{\bullet} + H^+ \quad (18)$$

Only PS/Ag, unlike PS/Fe and PS/Co, was confirmed to effectively generate SRs because Ag^+ activated a higher amount of PS within 48 h (0.15 M to 0.03 M, 80% consumption) while most of PS remained unused (0.15 M to 0.13 M, 13% consumption) in cases of Fe^{2+} and Co^{2+}. Ag-catalyzed quick PS activation is proposed to explain the observed PFAS decomposition in Fig. 4-2 and later Figs. 4-3 to 4-5 (Anderson and Kochi, 1970). Speciation of Ag during the reaction as well as its catalytic conversion are also important. Initial colorless solution with PFOA, PS, and Ag^+ at time 0 became dark and turned into black at around 60 sec and eventually back to colorless as seen in Fig. 4-3. We believe formation of Ag in higher oxidation states such as Ag^{2+}. More experiments

employing other transition metals at/in different oxidation states/groups, including gold (Au), nickel (Ni), copper (Cu), and iridium (Ir), should be conducted.

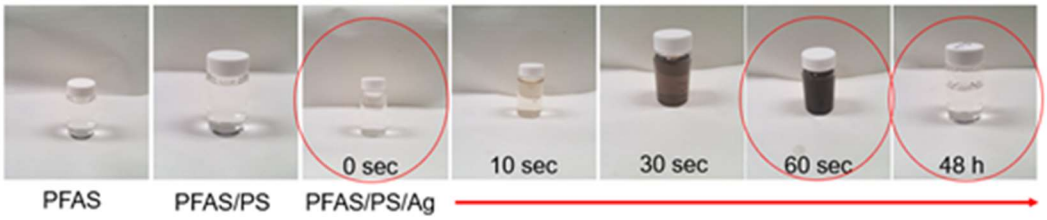

Figure 4-3: Change in color of the reaction solution in the silver persulfate system (10 mg/L PFOA, 0.6 mM Ag^+, 0.15 M PS, initial pH 4.5 to final pH around 1.5 (no pH control), temperature 20 °C)

Since PS was consumed fast in PS/Ag, adding enough amounts of PS were expected to show better decomposition of PFOA. This was confirmed in Table 4-1 summarizing defluorination of carboxylic PFAS under different PS/Ag ratios at 20 ˚C. Defluorination here describes detachment of fluorine caused by various reactions in a wide concept, not only reductive defluorination (direct attack and break of C-F bonds, releasing F^-) but also oxidation followed by mineralization by radical attack. For PFOA, increase in PS concentration from 0.15 M to 0.3 M at fixed Ag^+ of 0.6 mM showed much improved defluorination from 4.7% to 7.0%. However, further increase in PS from 0.3 M to 0.6 M did not improve much. Many previous studies have reported the presence of an optimum ratio of oxidants to metals because excessive amounts of metals and/or oxidants either prevent radical generation or quench generated radicals (Nfodzo and Choi, 2011). Indeed, increase in Ag concentration from 0.6 mM to 1.2 mM at fixed PS of 0.15 M showed rather a detrimental effect on PFOA decomposition, reducing defluorination from 4.7% to 4.1%.

Table 4-1: Defluorination of carboxylic PFAS under different PS/Ag ratios at 20 ℃.

PFAS	PS (M)	Ag^+ (mM)	F^- (mg/L) (mM)	Defluorination (%) [a]
PFNA [b]	**0.15**	**0.60**	**1.40 ± 0.09 (0.074)**	**20.1 ± 1.3**
PFNA	0.30	0.60	1.8 (0.095)	25.9
PFOA [b]	**0.15**	**0.6**	**0.32 ± 0.01 (0.017)**	**4.70 ± 0.15**
PFOA	0.15	1.20	0.28 (0.015)	4.1
PFOA	0.30	0.60	0.48 (0.025)	7.0
PFOA	0.60	0.60	0.52 (0.027)	7.5
PFHpA [b]	**0.15**	**0.60**	**0.12 ± 0.03 (0.006)**	**1.8 ± 0.45**
PFHpA	0.30	0.60	0.18 (0.009)	2.6

[a] Defluorination % is simply calculated, based on observed F^- ion concentration in comparison to maximum F^- ion concentration when all fluorines are detached (7 mg/L (0.368 mM) for PFNA, 6.9 mg/L (0.363 mM) for PFOA, and 6.8 mg/L (0.357 mM) for PFHpA).

[b] Standard conditions: 0.15 M PS and 0.6 mM Ag^+.

PS is one of strong oxidants known to generate highly reactive radicals such as SRs and superoxide radical anions (SRAs, $O_2^{\bullet-}$), along with HRs. In fact, SRs more selectively involve electron transfer in oxidation events because SRs have a higher oxidation potential at 2.3 V than HRs at 2.1 V (depending on pH), making them a slightly better species for the direct electron transfer for PFAS decomposition than HRs (Buxton et al., 1988; Neta et al., 1988; Neta et al., 1977). SRAs are also reported to reductively decompose PFOA (Da-Silva Rackov et al., 2016; Ahmad, 2012). No significant

decomposition of PFOA was observed in the presence of either TBA or methanol as radical scavengers (i.e., no observed decomposition; data is trivial to show), suggesting HRs may also contribute directly or indirectly to the reaction. Reflecting the result and considering that SRs are expected to be prevalent over HRs under the acidic conditions tested (Lee et al., 2012), both SRs and HRs (and presumably Ag^{2+}) seem to play a role in decomposing PFOA.

4.3.3 PFAS Decomposition in Comparison

Since the successful decomposition of PFOA was observed using PS/Ag at 20 ˚C, other PFAS (one sulfonic PFAS (i.e., PFOS) and three carboxylic PFAS with different carbon chain lengths) were also tested in comparison, as shown in Fig. 4-4. All carboxylic PFAS, namely PFNA, PFOA, and PFHpA, were decomposed significantly. As expected, longer chain PFAS showed greater decomposition, in order of PFNA at 83%>PFOA at 42%>PFHpA at 30%. However, decomposition of PFOS was not observed over 48 hr. This could be explained most probably by the selectivity of PS/Ag system to attack the carboxylic group in PFAS (Anderson and Kochi, 1970). PS under high temperatures at around 60−90 °C was also reported to decompose exclusively PFCA such as PFOA (Yang et al., 2020; Bruton and Sedlak, 2018 and 2017; Park et al., 2016). A recent study by dos Passos Gomes et al. (2019) suggested that C-S bond present in an alkyl chain such as PFOS requires a much higher external energy source to overcome the activation energy needed for its decomposition.

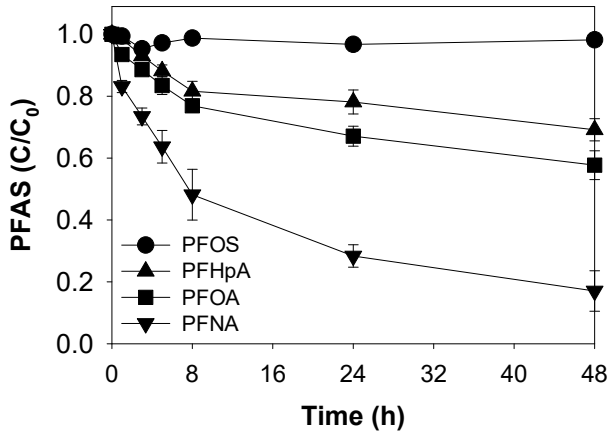

Figure 4-4: Decomposition of various PFAS (one sulfonic PFAS and three carboxylic PFAS) by PS conjugated with Ag^+ at room temperature (10 mg/L PFAS, 0.6 mM Ag^+, 0.15 M PS, initial pH 4.5 to final pH around 1.5 (no pH control), temperature 20 °C).

4.3.4 Fluoride Release and Byproduct Formation

Figure 4-5 shows evolution of fluoride ions released during the decomposition of carboxylic PFAS by PS/Ag at 20 °C and Table 4-1 summarizes calculated defluorination % based on fluoride ions found (please note actual defluorination % might be higher due to the potential escape of fluoride as hydrofluoric acid). Defluorination of PFAS was much slower than their decomposition shown in Fig. 4-5. PFNA showed highest defluorination at 20.1%, followed by PFOA at 4.7 % and PFHpA at 1.8% under the standard conditions. When concentration of PS was increased from 0.15 M to 0.3 M, defluorination % increased to 25.9% for PFNA, 7.0% for PFOA, and 2.6% for PFHpA.

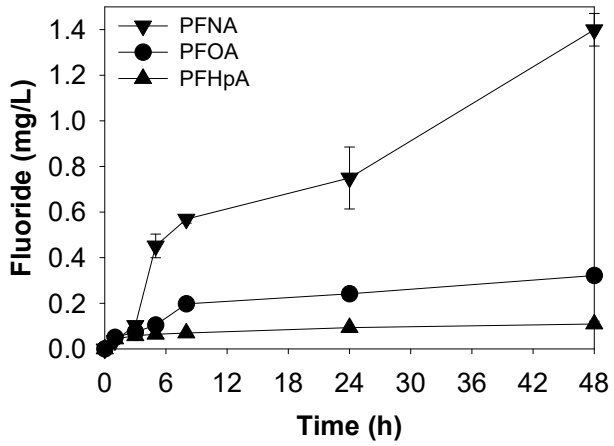

Figure 4-5: Evolution of fluoride ions released during the decomposition of carboxylic PFAS (PFNA, PFOA, PFHpA) by PS conjugated with Ag+ at room temperature (10 mg/L PFAS, 0.6 mM Ag+, 0.15 M PS, initial pH 4.5 to final pH around 1.5 (no pH control), temperature 20 °C). Maximum fluoride concentration, when all fluorines are detached, reaches 7.0, 6.9, and 6.8 mg/L for PFNA, PFOA, and PFHpA, respectively.

Figure 4-6 shows evolution of reaction byproducts. In all the cases, shorter chain PFAS were formed as identifiable PFAS through the targeted LC-MS analysis. For example, longest PFNA (9 carbons or C9) was decomposed to PFOA (C8), PFHpA (C7), PFHxA (C6), PFPeA (C5), and PFBA(C4). Significant decomposition of PFNA at 80% (from 10 mg/L (21.6 μM) to around 2.0 mg/L (4.32 μM)) was observed in 48 h while total identifiable byproducts (i.e., sum of C4-C8) accounted for only 4% (around 0.4 mg/L (1 μM)), implying formation of many other ill-defined intermediates and byproducts as well as possible mineralization of PFNA. Very similar result was reported by Bruton and Sedlak (2018), suggesting a systematic step-by-step removal of CF_2 moieties.

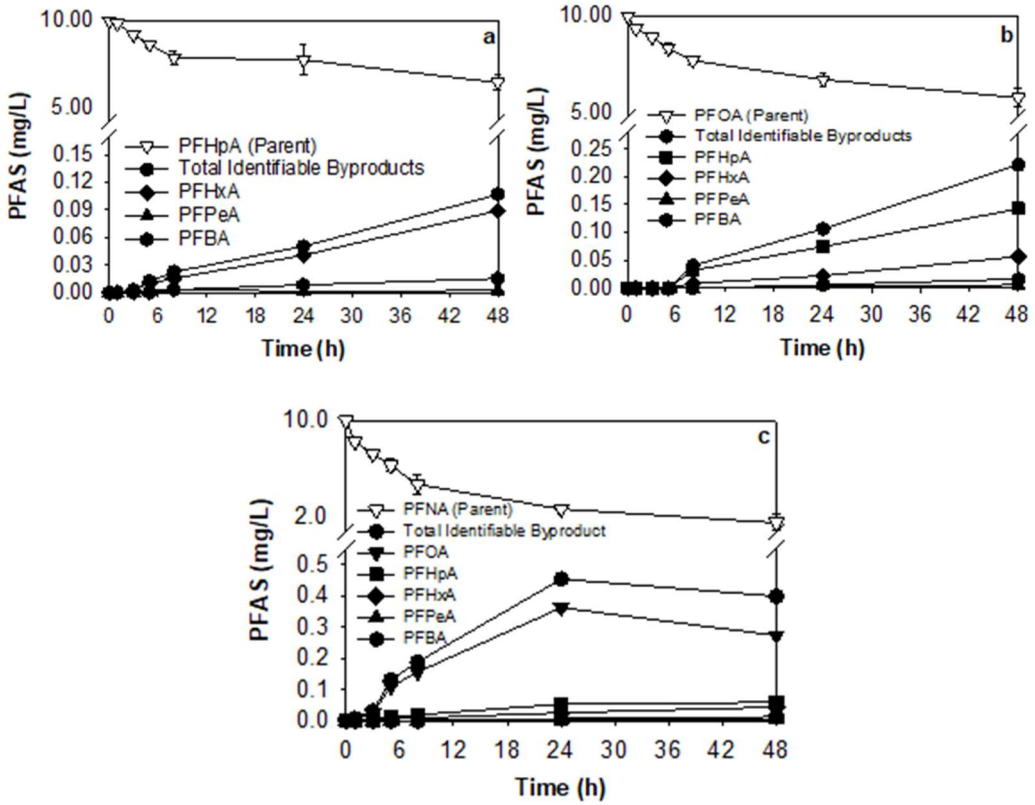

Figure 4-6: Evolution of reaction byproducts produced during the decomposition of carboxylic PFAS: (a) PFHpA, (b) PFOA, and (c) PFNA by PS conjugated with Ag+ at room temperature (10 mg/L PFAS, 0.6 mM Ag+, 0.15 M PS, initial pH 4.5 to final pH around 1.5 (no pH control), temperature 20 °C). Please note the number of identifiable byproducts (a few to several) found through targeted analysis is overwhelmed by that of unidentifiable byproducts.

4.4 Conclusions

The potential of the modified Fenton systems to decompose PFAS under ambient conditions was successfully demonstrated. Among many combinations of common oxidants and transition metals tested, PS/Ag pair showed significant reactivity at 20 ˚C exclusively towards carboxylic PFAS such as PFNA, PFOA, and PFHpA. However, sulfonic PFAS still remains challenging. Follow-up assignments are raised to i) investigate in-depth mechanism on PS/Ag reactivity to PFAS, ii) examine combinations of other oxidants and metals (e.g., Au, Ni, Cu, and Ir) at/in different oxidation states/groups, and iii) exploit transition metals even in zerovalent states (e.g., zerovalent Ag) and bimetallic particles (e.g., Ag/Fe). In addition, finding several best combinations of oxidants and transition metals should be followed by addressing post treatment issues such as recovery and disposal of transition metals (e.g., Ag is toxic to the environment). This study makes us one step-closer to establishing a less expensive, energy-independent, and more practical PFAS treatment system solely using chemical oxidants and metals.

4.5 References

Ahmad, A. (2012) Innovative Oxidation Pathways for the Treatment of Traditional and Emerging Contaminants, Doctoral Dissertation, Washington State University, Department of Civil Engineering and Environmental Engineering.

Anderson, J. M., Kochi, J. K. (1970). Silver (I) -catalyzed oxidative decarboxylation of acids by peroxydisulfate. The role of silver (II). J. Am. Chem. Soc. 92 (6). 1651-1659.

Anipsitakis, G. P., Dionysiou, D. D. (2004). "Radical generation by the interaction of transition metals with common oxidants." *Environ. Sci. Technol*. 38 (13), 3705–3712.

Bruton, T. A., Sedlak, D. L. (2018). Treatment of perfluoroalkyl acids by heat-activated persulfate under conditions representative of in situ chemical oxidation. Chemosphere 206, 457–464.

Bruton, T. A., Sedlak D. L. (2017). Treatment of aqueous film-forming foam by heat-activated persulfate under conditions representative of in situ chemical oxidation. Environ. Sci. Technol. 51(23): 13878-13885.

Buck, R. C., Franklin, J., Berger, U., Conder, J. M., Cousins, I. T., Voogt, P. De, Jensen, A. A., Kannan, K., Mabury, S. A., van Leeuwen, S. P. J. (2017). Perfluoroalkyl and polyfluoroalkyl substances in the environment: Terminology, classification, and origins. Integr. Environ. Assess. Manag. 7 (4): 513–541.

Buxton, G., Greenstock, C., Helman, W., Ross, A. (1988). Critical review of rate constants for reactions of hydrated electrons, hydrogen-atoms and hydroxyl radicals in aqueous solution. J. Phys. Chem. Ref. Data 17: 513-886.

Choi, H., Al-Abed, S.R., Dionysiou, D.D., Stathatos, E., Lianos, P. (2010). TiO2-Based Advanced Oxidation Nanotechnologies for Water Purification and Reuse. In I.I.

Escobar and A.I. Schafer, Eds., Sustainability Science and Engineering, Volume 2: Sustainable Water for the Future. 229-254. Elsevier Science: Netherlands.

Crawford, N. M., Fenton, S. E., Strynar, M., Hines, E. P., Pritchard, D. A., Steiner, A. Z. (2017). Effects of perfluorinated chemicals on thyroid function, markers of ovarian reserve, and natural fertility. Reprod. Toxicol. 69: 53–59.

Da Silva Rackov, C. K. O., Lawal, W. A., Nfodzo, P. A., Vianna, M., Do Nascimento, A., Choi, H. (2016). Decomposition of PFOA by hydrogen peroxide and persulfate activated by iron-modified diatomite. Appl. Catal. B: Environ. 192: 253-259.

Domingo, J. J., Nadal, M. (2017). Per-and Polyfluoroalkyl Substances (PFASs) in Food and Human Dietary Intake: A Review of the Recent Scientific Literature. J. Agric. Food Chem. 65: 533-543.

Dos Passos Gomes, G., Wimmer, A., Smith, A. M., Konig, B., Alabugin, I. V. (2019). CO2 or SO2: should it stay, or should it go? J. Am. Chem. Soc. 84 (10): 6232-6243.

Gong, Y., Lin, L. (2011). Oxidative decarboxylation of levulinic acid by silver(I)/persulfate. Molecules 16: 2714–2725.

Kissa, E. (1994). Fluorinated surfactants. Dekker, NY: Marcel Dekker Inc.

Lee, Y., Lo, S., Kuo, J., Hiseh, C. (2012). Decomposition of perfluorooctanoic acid by microwave-activated persulfate: Effects of temperature, pH, and chloride ions. Front. Environ. Sci. Eng. 6(1): 17-25.

Lee, Y. C., Lo, S. L., Chiueh, P. Te, Chang, D. G. (2009). Efficient decomposition of perfluorocarboxylic acids in aqueous solution using microwave-induced persulfate. Water Res. 43 (11): 2811–2816.

Liang, C., Huang, C. F, Mohanty, N., Kurakalva R. M. (2008). A rapid spectrophotometric determination of persulfate anion by ISCO. Chemosphere 73: 1540-1548.

Macheka-Tendenguwo, L. R., Olowoyo, J. O., Mugivhisa, L. L., Abafe, O. A. (2018). Per- and polyfluoroalkyl substances in human breast milk and current analytical methods. Environ. Sci. Pollut. 25: 36064–36086.

Merino, N., Qu, Y., Deeb, R. A., Hawley, E. L., Hoffmann, M. R., Mahendra, S. (2016). Degrading and removal methods for perfluoroalkyl and polyfluoroalkyl substances in water. Environ. Eng. Sci. 33: 615-649.

Neta, P., Huie, R. E., Ross, A. B. (1988). Rate constants for reactions of inorganic radicals in aqueous solution. J. Phys. Chem. Ref. Data 17: 1027.

Neta, P., Madhavan, V., Zemel, H., Fessenden, R. W. (1977). Rate constants and mechanisms of reaction of $SO_4^{\cdot-}$ with aromatic compounds. J. Am. Chem. Soc. 99 (1): 163-164.

Nfodzo, P., Choi, H. (2011). Triclosan decomposition by sulfate radicals: effects of oxidant and metal doses. Chem. Eng. J. 174, 629-634.

Parenky, A. C., Gevaerd de Souza, N., Asgari, P., Jeon, J., Nadagouda, M. N., Choi, H. (2020). Removal of perfluorooctanesulfonic acid (PFOS) in water by combining zerovalent iron particles with common oxidants. Environ. Eng. Sci. (In Press, DOI: 10.1089/ees.2019.0406).

Park, S., Lee, L. S., Medina, V. F., Zull, A., Waisner, S. (2016). Heat-activated persulfate oxidation of PFOA, 6:2 fluorotelomer sulfonate, and PFOS under conditions suitable for in-situ groundwater remediation. Chemosphere 145: 376–383.

Peluffo, M., Pardo, F., Santos, A., Romero, A. (2016). Use of different kinds of persulfate activation with iron for the remediation of a PAH-contaminated soil. Sci. Total Environ. 563–564: 649–656.

Rayne, S., Forest, K. (2009). Perfluoroalkyl sulfonic and carboxylic acids: A critical review of physicochemical properties, levels and patterns in waters and wastewaters, and treatment methods. J. Environ. Sci. Health A 44: 1145-1199.

Shaw, D. M. J., Munoz, G., Bottos, E. M., Duy, S. V., Sauvé, S., Liu, J., Van Hamme, J. D. (2019). Degradation and defluorination of 6:2 fluorotelomer sulfonamidoalkyl betaine and 6:2 fluorotelomer sulfonate by Gordonia sp. strain NB4-1Y under sulfur-limiting conditions. Sci. Total Environ. 647: 690–698.

United States Environmental Protection Agency (USEPA). (2016). US Environmental Protection Agency, Drinking Water Health Advisories for PFOA and PFOS (EPA-HQ-OW-2014-0138, FRL-9946-91-OW). Washington, DC: Office of the Federal Register, National Archives and Records Administration (NARA). Accessed on March 15, 2020.

United States Environmental Protection Agency (USEPA). (2009). EPA PFAS Drinking Water Laboratory Methods: Method 537: Determination of Selected Perfluorinated Alkyl Acids in Drinking Water by Solid Phase Extraction and Liquid Chromatography/Tandem Mass Spectrometry (LC/MS/MS). Accessed on May 8, 2020.

Vecitis, C., Park, H., Cheng, J., Mader, B., Hoffman, M. (2009). Treatment technologies for aqueous perfluorooctanesulfonate (PFOS) and perfluorooctanoate (PFOA). Front. Environ. Sci. Eng. 3: 129-151.

Wacławek, S., Lutze, H. V., Grübel, K., Padil, V. V. T., Černík, M., Dionysiou, D. D. (2017). Chemistry of persulfates in water and wastewater treatment: A review. Chem. Eng. J. 330: 44–62.

Wang, J., Wang, S. (2018). Activation of persulfate (PS) and peroxymonosulfate (PMS) and application for the decomposition of emerging contaminants. Chem. Eng. J. 334: 1502-1517.

Yang, L., He, L., Xue, J., Ma, Y., Xie, Z., Wu, L., Huang, M., Zhang, Z. (2020). Persulfate-based decomposition of perfluorooctanoic acid (PFOA) and perfluorooctane sulfonate (PFOS) in aqueous solution: Review on influence, mechanism and prospective. J. Hazard. Mater. 393: 122405.

Zhang, Y., Liu, J., Moores, A., Ghoshal, S. Forthcoming. Transformation of 6:2 fluorotelomer sulfonate by cobalt(II)-activated peroxymonosulfate. Environ. Sci. Technol. (In Press at https://doi.org/10.1021/acs.est.9b07113).

Chapter 5

Recommendations for future studies

This dissertation details some of the reductive/oxidative methods that were investigated for the removal and decomposition of per- and polyfluoroalkyl substances. In these studies reactions were conducted in ultrapure water, future studies should explore the role of organic matter by conducting experiments in field samples. The successful decomposition of carboxylic PFAS by the silver-persulfate system raises certain questions as to the role of silver (Ag) in activating and its possible behaviour as a catalyst. It would be important to understand the silver species (Ag^{0}, Ag^{+1} or Ag^{+2}) that is responsible for the decomposition. Simultaneously, the catalytic behaviour of the Ag species should be evaluated through sequential addition of oxidants. Although carboxylic-PFAS was successful degraded under ambient conditions, sulfonic PFAS still remain a challenge. Follow up studies investigating various other metal-oxidant combinations could potentially decompose PFAS and help in developing a comprehensive practical treatment technology.

Biographical Information

Akshay Parenky began his academic journey in India, where he earned his bachelor's degree in Chemical Engineering from the renowned University of Mumbai, Maharashtra. After a brief period working in the industry, he joined The University of Texas at Arlington (UTA) to pursue a master's degree in Engineering Management. Akshay continued his graduate studies at UTA in the Civil Engineering Ph.D. program where he could pursue his main interest: environmental remediation. His research focus involved the removal and decomposition of per- and polyfluoroalkyl substances via advanced oxidation techniques. He has worked on project that were funded by the Strategic Environmental Research and Development Program, Water Research Foundation and UTA. Over the course of his research, he has published several articles in journals such as Environmental Engineering Science and Journal of Environmental Engineering. Simultaneously, he has also participated in many local and national conferences to present his research. A long-term goal of his is to secure a position in the industry that involves applying some of the acquired skills and knowledge in real world environment.